We thank the two anonymous referees for their valuable comments and constructive suggestions on the manuscript. Below, we explain how the comments and suggestions are addressed and make note of the revision we made in the manuscript.

Anonymous Referee #1

General comments:

- ***This study investigates the impact of different land surface parameterizations and vegetation distributions on emissions and mixing ratios of biogenic VOCs (and related oxidation products) simulated in California. Isoprene, MACR, MVK and monoterpenes are especially considered. Two different versions of the Model of Emissions of Gases and Aerosols from Nature (MEGAN v2.0 and MEGAN v2.1), together with two different land surface schemes (Noah and CLM4.0) and 5 different vegetation distributions (VEGM, USGS, VEG1, VEG2, VEG3) are alternatively used. Data collected during two field campaigns, CalNex and CARES, providing ground-based or flight observations, are also considered for model evaluation.***

  This manuscript is well written and clearly presents an extensive work, which I really enjoyed reading, a work that provides clues to better understand the variability and uncertainty of biogenic VOC estimates between models. To some extent, the manuscript lacks of precise information, especially regarding the model framework. For example, the differences in emission calculation between the two versions of MEGAN used, or the connexions between the emission model and the land-surface scheme should be better described, in order to fully understand the possible source of variability in results provided. I therefore give a list of corrections and comments to improve the clarity of the manuscript, which I warmly recommend for publication in GMD.

We thank the reviewer for a detail review. Both text and figures are revised as the reviewer suggested.

Specific comments:

- ***Section 2.2 and 2.3:***

  These sections lack of clear information regarding the differences between the emission models or land-surface schemes, and connexions between them. First if CLM4 considers 16 PFTs, how many are taken into account in Noah?

Noah uses the 24 USGS land-use types. We have modified the text to include "Noah has four soil layers, with a total depth of two meters and a single slab snow layer that is lumped with the top-soil layer, which is set to a combined depth of 10 cm. It uses the 24 United States Geological Survey (USGS) land-use types, and does not treat sub-grid scale variability within a model grid cell."

More clarification is added into Section 2.2 and 2.3 as indicated in the responses to the comments below.

- ***From page 9, lines 199-203, it is not really clear to me which meteorology is considered when using MEGAN v2.0: is it eventually provided by WRF-CHEM or***

based on a monthly climatology?

MEGAN v2.0 in WRF-Chem needs instantaneous and past-days' mean meteorological variables that are from the WRF-Chem simulation and the monthly climatology dataset, respectively. We have modified the text to state "The biogenic emission calculation in MEGAN uses both instantaneous and the past-days' surface air temperature and solar radiation. MEGAN v2.0 obtains the instantaneous value from the land surface parameterization and the past-days' value from the climatological monthly mean dataset. In contrast, MEGAN v2.1 obtains both values directly from CLM."

- ***Differences in emission schemes between MEGAN 2.0 and MEGAN 2.1 should also be more precisely stated in the text regarding number of vegetation classes, emission factors (are they prescribed for each PFT for both MEGAN v2.0 and MEGAN v2.1 or is one using EF maps?).***

The text has been modified to include "In this study, both MEGAN v2.0 and v2.1 estimate biogenic species emissions based on the PFT distributions and the PFT specific emission factors. MEGAN v2.0 and v2.1 use 4 and 16 PFTs, respectively, as described below in Section 2.4."

- ***Connexions and variables coupling between emission model and land-surface scheme (any version) should be given in details: which of the variables calculated by the landsurface scheme are actually used in MEGAN v2.0 and v2.1 to calculated emissions? This is also especially important in section 4, when analyzing the impact of using different land-surface parameterizations.***

We have modified the text to say "In the released version, MEGAN v2.0 can be used with any land surface scheme available in WRF-Chem including Noah and CLM4." and "The biogenic emission calculation in MEGAN uses both instantaneous and the past-days' surface air temperature and solar radiation. MEGAN v2.0 obtains the instantaneous value from the land surface parameterization and the past-days' value from the climatological monthly mean dataset. In contrast, MEGAN v2.1 obtains both values directly from CLM." In section 4, we have revised the discussion in the following text: "Although the two land surface parameterizations produce slightly different values of surface temperature (Fig. 1), soil moisture (not shown), and net solar radiation near the surface (not shown), their impact on the biogenic emissions was small." and "Although both experiments with Noah and CLM4 (red and orange lines, respectively) simulate similar isoprene emission fluxes with the maximum in the afternoon (Fig. 10), their respective isoprene+MVK+MACR mixing ratios are different at the four sites, particularly at site T0, where the Mv20CLM simulated isoprene+MVK+MACR mixing ratios during the daytime are about a factor of 2 larger than those from Mv20Noah. This inconsistence mainly results from the differences in the near surface meteorology, such as net surface radiation and temperature, between the two experiments (not shown) that

affects photochemistry, but this impact of surface meteorology occurs only at limited locations."

- ***Finally, nothing is said anywhere in the manuscript about the leaf area index, which is yet a crucial driving variable in emission estimate in MEGAN. How is it taken into account: is LAI prescribed or is it calculated by each land-surface scheme, and if so what are the LAI differences or similarities between them?***

The leaf area index is prescribed using the 4 PFTs in MEGAN2.0 and 16 PFTs in MEGAN2.1. Figure 6 has been added to show the difference in LAI among the experiments and the following description has been added to the text: "Figure 6 shows the spatial distributions of LAI used in MEGAN v2.0 and v2.1. The differences in the spatial distributions of LAI can significantly affect the biogenic emission calculation in MEGAN. It should be noted that in MEGAN v2.0 used in WRF-Chem, the LAI used for the calculation of the biogenic emissions is prescribed using the 4 PFTs, which is different than the land scheme that uses the LAI derived from the 24 USGS land categories."

- ***Page 9, lines 186-194: please also specify here in the text that MEGAN v.2.0 considers 4 PFTs only.***

Done, we have revised the text to say "MEGAN v2.0 and v2.1 use 4 and 16 PFTs, respectively, as described below in Section 2.4."

- ***Results from both MEGAN v2.0 and v2.1 are eventually compared with each other, and with observations. Is this comparison actually consistent since MEGAN v2.0 emission factors represent the net emission flux into the atmosphere, and MEGAN v2.1 ones the net primary emission that escape into the atmosphere? Are there significant differences between the two set of emission factors? MEGAN v2.0 emission factors should also be given, as is done for MEGAN v2.1 in figure 3. Ideally, maps of emission factors, projecting emission factor values over PFT distribution, would really help understanding the differences between both emission models.***

The difference in the definition (net flux versus primary emission) of emission factors affects the emission factors of compounds with bidirectional exchange but does not impact MEGAN isoprene and monoterpene emission factors because they have small deposition rates relative to emission rates. We have revised the text to state "The difference in the definition (net flux versus primary emission) of emission factors affects the emission factors of compounds with bidirectional exchange but does not impact MEGAN isoprene and monoterpene emission factors because they have small deposition rates relative to emission rates."

Figure 4 has been revised to include the biogenic isoprene emission factor for the 4 PFTs used in MEGAN v2.0. Figure 5 has been added to show the differences in the spatial distributions of averaged biogenic isoprene emission factor in MEGAN v2.0 and v2.1 with different PFTs. The text is revised as "Figure 4 shows the biogenic isoprene emission factor for each PFT prescribed in MEGAN v2.0 and MEGAN v2.1 in CLM4. In MEGAN v2.1, it shows that temperate broadleaf deciduous tree (PFT 7 listed in Table 1) has a large isoprene emission factor, while temperate needleleaf evergreen tree (PFT 1 listed in Table 1) has a small isoprene emission factor. A similar difference between broadleaf trees and needleleaf trees is indicated for MEGAN v2.0. Figure 5 shows the spatial distributions of averaged biogenic isoprene emission factor used in MEGAN v2.0 and v2.1 with different PFTs. It is evident that the difference in the distributions of PFTs results in a significant difference in spatial distributions of the isoprene emission factor."

Technical corrections:

- ***Page 3, line 69; page 4, line 74; page 5, line 105: change "BVOCs" to "BVOC"***

Corrected.

- ***Page 5, line 100: change "during the day but a factor of three" to "during the day but by a factor of three"***

Corrected.

- ***Page 7, line 145: please write what RRTMG stands for***

Corrected.

- ***Page 8, line 172: change "PFT's to "PFTs"***

Corrected.

- ***Page 9, line 191: change "defined" to "defines"***

Corrected.

- ***Page 10, line 215: change "MEGAN to "MEGAN v2.1***

Corrected.

- ***Page 12, line 276: change "PFT's" to "PFTs"***

Corrected.

- ***Page 14, line 312: change "BVOCs simulation" to "BVOC simulation"***

Corrected.

- ***Page 18, line 396: change "monterpene" to "monoterpene"***

Corrected.

- ***Page 19, line 422: change "and monoterpene" to "and monoterpenes"***

Corrected.

- ***Page 19, line 423: add "and Figure 13" (for monoterpenes) after "Figure 12" Page***

Corrected.

- ***21, line 463-464: change "while both experiments are slightly smaller" to "while both experiment mixing ratios are slightly smaller"***

Corrected.

- ***Page 28, line 634: change "and hence the atmospheric VOC mixing ratios" to "and hence of atmospheric VOC mixing ratios"***

Corrected.

- ***Page 30, lines 688, 689 and 690: change "BVOCs emission" to "BVOC emission"***

Corrected.

- ***Page 31, line 701: change "v20" and "v21" (twice) to "v2.0" and "v2.1" respectively***

Corrected.

- ***Page 41, line 915: the font used for "Müller J." seems different to me than the one used for the rest of the text***

Corrected.

- ***Table 1 and Figure 2 captions: change "PFT's" to "PFTs"***

Corrected.

- ***Figure 12, bottom left plot: Is actually isoprene mixing ratio plotted or isoprene+MVK+MACR?***

It is isoprene. Now it is clarified as "At the Bakersfield site, only isoprene mixing ratios were reported so that the comparison is for isoprene only."

Anonymous Referee #2

General comments:

- ***This is an excellent paper and it should make a significant contribution to GMD. Because it will serve as a reference for users of the widely used community modeling system WRF-Chem, I agree with comments from reviewer #1 that it requires a bit more information and precision. In addition to the comments from the other reviewer, I would like to see more details and clarification on the following points.***

We thank the reviewer for a detailed review. Both text and figures are revised as the reviewer suggested.

Specific comments:

- ***(1) The authors apply nudging. While is appropriate for their application in which they only look at the sensitivity of biogenic emissions to land surface parameterizations and vegetation distributions, the reader should have a little bit more info. Is the nudging also applied in the Boundary Layer (BL) and at the surface? Why did you choose not to nudge moisture? I would not expect the answers to this question to alter the quality of the results.***

The nudging is only applied in the free atmosphere above the BL. In general, we do not nudge moisture because we want the model to freely simulate clouds. As the reviewer also points out, the nudging method should not lead to changes of our results. It is now clarified in the text as "The modeled u and v wind components and temperature in the free atmosphere above the planetary boundary layer are nudged towards the NARR reanalysis data with a time scale of 6 hours [Stauffer and Seaman, 1990]."

- ***(2) I would have been interested to get a bit more info on the difference in surface meteorology, assuming that nudging was not applied in the BL. What was the relative impact from meteorology compared to land-use and/or a different version of MEGAN? Of course, if nudging was applied in the BL this would be a moot point. If the authors can elaborate a little on this that could be useful.***

In this manuscript we have not focused on the meteorological impact. There are small differences in the surface meteorological fields among the experiments, for example, there are differences in latent heat and sensible heat fluxes. However, as we discussed in the text that the impact of surface meteorological difference on biogenic emissions is relatively small compared to the vegetation impact. For example in the text, "Although the two land surface parameterizations produce slightly different values of surface temperature (Fig. 1), soil moisture (not shown), and net solar radiation near the surface (not shown), their impact on the biogenic emissions was small."

We also discussed about the potential impact of surface meteorology on surface mixing ratios. The text as been modified as follows, "Although both experiments with Noah and

CLM4 (red and orange lines, respectively) simulate similar isoprene emission fluxes with the maximum in the afternoon (Fig. 10), their respective isoprene+MVK+MACR mixing ratios are different at the four sites, particularly at site T0, where the Mv20CLM simulated isoprene+MVK+MACR mixing ratios during the daytime are about a factor of 2 larger than those from Mv20Noah. This inconsistence mainly results from the differences in the near surface meteorology, such as net surface radiation and temperature, between the two experiments (not shown) that affects photochemistry, but this impact of surface meteorology occurs only at limited locations."

- ***(3) I assume this was a dry period in the model simulations, so slight differences in cloud distributions could not have contributed much to the differences between model simulations in this case. However, could this have played a role in under/over forecasting for simulations of all runs in general?***

Yes, this study during a dry and warm period that favors biogenic emissions. For a more general case, the absolute impact may be smaller. The more quantitative conclusion should be drawn with multiple-season simulation in future studies. This is now acknowledged in the discussion section, where the text has been modified to read "It is also noteworthy that this study is in a relatively dry and warm season; therefore the impact of biogenic emission treatments may change for other seasons and during periods with higher cloudiness. A multiple-season investigation may be needed in future."

Sensitivity of biogenic volatile organic compounds (BVOCs) to land surface parameterizations and vegetation distributions in California

[1]Chun Zhao, [1]Maoyi Huang, [1]Jerome D. Fast, [1]Larry K. Berg, [1]Yun Qian, [2]Alex Guenther, [2]Dasa Gu, [1]Manish Shrivastava, [1]Ying Liu, [3]Stacy Walters, [3]Gabriele Pfister, [4]Jiming Jin, [1]John E. Shilling, [5,6]Carsten Warneke

[1]*Atmospheric Science and Global Change Division, Pacific Northwest National Laboratory, Richland, WA, USA*

[2]*Department of Earth System Science, University of California, Irvine, California, USA*

[3]*National Center for Atmospheric Research, CO, USA*

[4]*Departments of Watershed Sciences and Plants, Soils, and Climate, Utah State University, Logan, UT, USA*

[5]*National Oceanic and Atmospheric Administration, Earth System Research Laboratory, USA*

[6]*CIRES, University of Colorado, Boulder, CO, USA*

Manuscript for submission to *WRF-Chem special issue in Geosci. Model Dev.*

*Corresponding author: Chun Zhao, phone: (509) 371-6372; email: chun.zhao@pnnl.gov

Abstract. Current climate models still have large uncertainties in estimating biogenic trace gases, which can significantly affect atmospheric chemistry and secondary aerosol formation that ultimately influences air quality and aerosol radiative forcing. These uncertainties result from many factors, including uncertainties in land-surface processes and specification of vegetation types, both of which can affect the simulated near-surface fluxes of biogenic volatile organic compounds (BVOCs). In this study, the latest version of Model of Emissions of Gases and Aerosols from Nature (MEGAN v2.1) is coupled within the land surface scheme CLM4 in the Weather Research and Forecasting model with chemistry (WRF-Chem). In this implementation, MEGAN v2.1 shares a consistent vegetation map with CLM4 for estimating BVOC emissions. This is unlike MEGAN v2.0 in the public version of WRF-Chem that uses a standalone vegetation map that differs from what is used by land surface schemes. This improved modeling framework is used to investigate the impact of two land surface schemes, CLM4 and Noah, on BVOCs and examine the sensitivity of BVOCs to vegetation distributions in California. The measurements collected during the Carbonaceous Aerosol and Radiative Effects Study (CARES) and the California Nexus of Air Quality and Climate Experiment (CalNex) conducted in June of 2010 provide an opportunity to evaluate the simulated BVOCs. Sensitivity experiments show that land surface schemes do influence the simulated BVOCs, but the impact is much smaller than that of vegetation distributions. This study indicates that more effort is needed to obtain the most appropriate and accurate land cover datasets for climate and air quality models in terms of simulating BVOCs, oxidant chemistry, and consequently secondary organic aerosol formation.

1. Introduction

Volatile organic compounds (VOCs) in the atmosphere play an important role in atmospheric chemistry, and therefore can significantly affect ozone and secondary organic aerosol (SOA) formation and ultimately air quality and climate [e.g., Chameides et al., 1992; Fehsenfeld et al., 1992; Andreae and Crutzen, 1997; Pierce et al., 1998; Poisson et al., 2000; Sanderson et al., 2003; Claeys et al., 2004; Arneth et al., 2010]. Significant effort has been made on obtaining accurate predictions of atmospheric VOC concentrations; however, there remain large differences between observed and simulated values. These uncertainties result from many factors, including biogenic emission rates that are influenced by near-surface meteorological processes, sub-surface processes, representation of vegetation distributions, and plant biology [Guenther et al., 2013].

Biogenic emissions are a major source of VOCs [e.g., Zimmerman et al., 1978; Mueller, 1992] in the atmosphere. In particular, isoprenoids (consisting mainly of isoprene and monoterpenes) that dominate biogenic VOCs (BVOCs) have been extensively investigated during the last five decades [e.g., Went, 1960; Rasmussen, 1972; Zimmerman et al., 1979; Lamb et al., 1987; Pierce et al., 1998; Niinemets et al., 1999 and 2002; Arneth et al., 2007; Schurgers et al., 2009; Guenther et al., 1995 and 2012]. BVOC emissions were originally computed offline, producing prescribed emission inventories used by regional and global models [e.g., Huang et al., 2011]. However, emissions of BVOCs depend on diurnal, multi-day, and seasonal variations in light intensity, temperature, soil moisture, vegetation type, and leaf area index (LAI) [e.g., Pierce et al., 1998; Niinemets et al., 1999 and 2002; Arneth et al., 2007; Schurgers et al., 2009; Guenther et al., 2012]. Therefore, various BVOC emission algorithms have been

Chun Zhao 4/29/2016 10:40 AM
Deleted: BVOCs

proposed that extrapolate limited laboratory and field measurements to prescribed regional and global ecosystems [e.g., Pierce et al., 1998; Niinemets et al., 1999 and 2002; Arneth et al., 2007; Schurgers et al., 2009; Guenther et al., 1995 and 2012]. The uncertainties in biogenic emission schemes are mainly due to the scarcity of observations of BVOC fluxes and vegetation distributions over regional scales. Inappropriate coupling strategies between biogenic emission and land-surface schemes may also introduce errors in estimating atmospheric BVOCs. For example, some models specify different vegetation distributions for biogenic emissions and land-atmosphere interaction processes as applied in different parts of models.

Chun Zhao 4/29/2016 10:40 AM
Deleted: BVOCs

BVOCs play a significant role in affecting the air quality and regional climate over California, where there have been many studies, such as the Carbonaceous Aerosol and Radiative Effects Study (CARES) [Zaveri et al., 2012] and the California Nexus of Air Quality and Climate Experiment (CalNex) [Ryerson et al., 2013], investigating the impacts of BVOCs and their interaction with anthropogenic pollutants. In the past 20 years, California's economy has grown rapidly and the population has increased by 33% [Cox et al., 2009]. Although California has reduced the emissions of most primary pollutants, poor air quality still affects the well-being of millions of people. Nearly all Californians live in areas that are designated as nonattainment for the state (about 99%) and national (about 93%) health-based O_3 and/or PM standards. Accurate predictions of O_3 and PM concentrations are needed to develop effective attainment strategies, but this is complicated, in part, due to uncertainties associated with long-range transport of pollutants and local natural emission sources such as BVOCs.

In California, the complex topography and distribution of vegetation makes it

94 difficult for models to capture the variability of BVOCs at regional and local scales. For
95 example, Fast et al. [2014] showed that simulated biogenic emissions varied by as much
96 as a factor of 2 within 8 km of an observation site in Cool, California. They also found
97 that daytime mixing ratios of isoprene and monoterpenes from a regional simulation
98 using the Weather Research and Forecasting model with chemistry (WRF-Chem) [Grell
99 et al., 2005; Fast et al., 2006] are usually a factor of two smaller than the observations
100 collected both at the rural Cool site and an urban Sacramento site. Conversely, simulated
101 monoterpene mixing ratios were similar to observations during the day but by a factor of
102 three too high at night at the observation site in Cool. They suggested that the biogenic
103 emission rates calculated based on the Model of Emissions of Gases and Aerosols from
104 Nature version 2.0 (MEGAN v2.0) might contribute to major biases in their simulations.
105 Knote et al. [2014] also found that their simulations using WRF-Chem with MEGAN
106 v2.0 produced BVOC concentrations that were too small over Los Angeles, and
107 suggested that there might be deficiencies in the description of vegetation in urban areas.
108 Thus, it is evident that uncertainties in simulated atmospheric BVOCs can arise from how
109 well vegetation is represented in models. Furthermore, to our knowledge, none of the
110 numerous chemical transport modeling studies for California have investigated the
111 sensitivity of BVOC simulations to land surface schemes and vegetation distributions.
112 To better understand the uncertainties in simulating BVOCs associated with land
113 surface schemes and vegetation distributions in California, the latest version of MEGAN
114 (MEGAN v2.1) is coupled into the CLM4 land surface scheme of WRF-Chem in this
115 study. Multiple sensitivity experiments are conducted using this improved modeling
116 framework at a relatively high spatial resolution to capture the region's complex

Chun Zhao 4/29/2016 10:40 AM
Deleted: BVOCs

topography and vegetation distribution. Simulations are conducted using WRF-Chem with "fully" coupled version of CLM4 and MEGAN v2.1 (i.e., CLM4 and MEGAN share a consistent vegetation dataset) and compared with the measurements collected during CARES and CalNex conducted in June 2010. This new coupling also adds the capability of quantifying the impact of different vegetation distributions on simulating BVOCs. Simulations are also performed using two land surface schemes (Noah and CLM4) coupled with MEGAN v2.0. As with previous studies using WRF-Chem, MEGAN v2.0 uses a different vegetation dataset from the land surface schemes. The WRF-Chem experiments with MEGAN v2.0 and MEGAN v2.1 are included together here as a reference for future studies in the community and for users interested in migrating from the widely used v2.0 to v2.1.

The rest of manuscript is organized as follows. Sections 2 and 3 describe the WRF-Chem model and the observations used in this study, respectively. The sensitivity of modeling BVOCs to the land surface schemes and the vegetation distributions are analyzed in section 4. The findings are then summarized and discussed in section 5.

2. Model Description and Experimental Design

2.1 WRF-Chem

The WRF-Chem (v3.5.1) configuration is similar to that used by Fast et al. [2014] for studying aerosol evolution over California, except that this study excludes aerosols and focuses on simulated BVOCs. The model includes numerous options for the treatment of physics and chemistry processes. In this study, the SAPRC-99 photochemical mechanism [Carter, 2000a,b] is selected to simulate gas-phase chemistry,

and the Fast-J parameterization [Wild et al., 2000] for photolysis rates. For all the simulations in this study, we use the Yonsei University (YSU) parameterization [Hong et al., 2006] for the planetary boundary layer (PBL), the Monin-Obukhov similarity theory [Paulson, 1970] to represent the surface layer, the Morrison two-moment parameterization [Morrison et al., 2009] for cloud microphysics, the Kain-Fritsch parameterization [Kain 2004] for sub-grid scale clouds and precipitation, the rapid radiative transfer parameterization (RRTMG) for longwave and shortwave radiation [Iacono et al., 2008]. Since Fast et al. [2014] has evaluated the simulated meteorological fields and gases and aerosols with a similar model configuration, this study will focus primarily on the BVOC simulation.

Chun Zhao 4/29/2016 10:40 AM
Deleted: RRTMG

Chun Zhao 4/29/2016 10:40 AM
Deleted: BVOCs

2.2 Land surface schemes

Two land surface schemes, Noah and CLM4.0, are used to quantify how differences in the treatment of land surface processes, including latent and sensible heat fluxes, soil moisture, and surface albedo, affect near-surface meteorological conditions and consequently simulated BVOC emissions and concentrations. The Noah land surface scheme, described by Barlage et al. [2010] and LeMone et al. [2010a, 2010b], has been used in numerous studies with WRF-Chem. Noah has four soil layers, with a total depth of two meters and a single slab snow layer that is lumped with the top-soil layer, which is set to a combined depth of 10 cm. It uses the 24 United States Geological Survey (USGS) land-use types, and does not treat sub-grid scale variability within a model grid cell.

Chun Zhao 4/29/2016 10:40 AM
Deleted: Noah

The CLM4 (Community Land Model version 4.0) [Lawrence et al. 2011; Jin et al., 2012] was recently coupled and released with WRF (since v3.5) as one of the land surface scheme options. CLM4 in global and region applications has been shown to be

Chun Zhao 4/29/2016 10:40 AM
Deleted: (CLM4

accurate in describing snow, soil, and vegetation processes [Zeng et al., 2002; Jin and Miller, 2007; Zhao et al., 2014]. CLM4 includes five layers for snow, 10 layers for soil, and a single-layer for vegetation. The soil is divided into 19 categories defined according to percentages of sand and clay. The two-stream approximation [Dickinson, 1983] is applied to vegetation when calculating solar radiation reflected and absorbed by the canopy as well as radiation transfer within the canopy. Each model grid cell can be divided into a maximum of 10 smaller cells to account for sub-grid scale heterogeneity and its impact on the land surface processes. The 24 USGS land-use types are mapped to the 16 plant functional types (PFTs) in CLM4 based on a lookup table derived from Bonan et al. [1996]. Additional technical details of CLM4 are provided in Oleson et al. [2004].

Chun Zhao 4/29/2016 10:40 AM
Deleted: United States Geological Survey (

Chun Zhao 4/29/2016 10:40 AM
Deleted:)

Chun Zhao 4/29/2016 10:40 AM
Deleted:

Chun Zhao 4/29/2016 10:40 AM
Deleted: PFT's

2.3 MEGAN and coupling with CLM4

MEGAN is a modeling framework for estimating fluxes of biogenic compounds between terrestrial ecosystems and the atmosphere using simple mechanistic algorithms to account for the major known processes controlling biogenic emissions [Guenther et al., 2006, 2012]. Two versions (v2.0 and v2.1) of MEGAN are used in this study. MEGAN v2.1 is an update from MEGAN v2.0 [Guenther et al., 2006; Sakulyanontvittaya et al., 2008] that includes additional compounds, emission types, and controlling processes. MEGAN v2.1 estimates emissions (F_i) for 19 compound classes (i) from terrestrial landscapes based on emission factors ($\varepsilon_{i,j}$) at standard conditions for vegetation type j with fractional grid box areal coverage χ_j, i.e., $F_i = \gamma_i \Sigma \varepsilon_{i,j} \chi_j$, where γ_i is emission activity factor from the processes controlling emission responses to environmental and phenological conditions [Guenther et al., 2006, 2012].

For emission factors, MEGAN v2.0 enabled users to customize vegetation emission type schemes ranging from detailed (e.g. individual plant species or sub species) to generic (e.g. a few broad vegetation categories). MEGAN2.1 emission factors can be specified from gridded maps based on species composition and species-specific emission factors or by using PFT distributions and the PFT specific emission factors. MEGAN2.0 defines emission factors as the net flux of a compound into the atmosphere, while MEGAN2.1 emission factor represents the net primary emission that escapes into the atmosphere but is not the net flux because it does not include the downward flux of chemicals from above canopy. The difference in the definition (net flux versus primary emission) of emission factors affects the emission factors of compounds with bidirectional exchange but does not impact MEGAN isoprene and monoterpene emission factors because they have small deposition rates relative to emission rates. In this study, both MEGAN v2.0 and v2.1 estimate biogenic species emissions based on the PFT distributions and the PFT specific emission factors. MEGAN v2.0 and v2.1 use 4 and 16 PFTs, respectively, as described below in Section 2.4.

The publically available version of WRF-Chem includes the MEGAN v2.0 scheme for calculating BVOC emission fluxes (WRF-Chem user guide: http://ruc.noaa.gov/wrf/WG11/Users guide.pdf). It has been widely used for gas and aerosol simulations [e.g., Shrivastava et al., 2011, 2013; Gao et al., 2011, 2014; Knote et al., 2014; Fast et al., 2014]. In the released version, MEGAN v2.0 can be used with any land surface scheme available in WRF-Chem including Noah and CLM4. However, MEGAN v2.0 was originally not coupled into the land surface scheme in WRF-Chem (since v3.1). The biogenic emission calculation in MEGAN uses both instantaneous and

Chun Zhao 4/29/2016 10:40 AM
Deleted: defined

Chun Zhao 4/29/2016 10:40 AM
Deleted:), and used the climatological monthly mean surface air temperature and solar radiation to represent the values for last few days for

Chun Zhao 4/29/2016 10:40 AM
Deleted: that needs

Chun Zhao 4/29/2016 10:40 AM
Deleted: values

the past-days' surface air temperature and solar radiation. MEGAN v2.0 obtains the instantaneous value from the land surface scheme and the past-days' value from the climatological monthly mean dataset. In contrast, MEGAN v2.1 obtains both values directly from CLM. Figure 1 shows the example of the comparison between the input climatological and model simulated monthly mean surface air temperature in June. It is apparent that the monthly-averaged simulated surface air temperature is much different from the climatology value. In addition, the vegetation dataset (referred to as VEG-M, will be discussed in Section 2.4) used in MEGAN v2.0 for calculating BVOC emission fluxes is also different from the one used by the land surface scheme, which allows MEGAN v2.0 to be used with any of the available land surface schemes (e.g., Noah and CLM4) in WRF-Chem. This inconsistency in vegetation distributions may introduce errors in simulating emissions and concentrations of BVOC. To avoid this inconsistency, we have coupled MEGAN v2.1 with WRF-Chem embedded in the CLM4 land surface scheme. Therefore, the coupling of MEGAN v2.1 and CLM4 in WRF-Chem now has the same functionality as CLM4 in the Community Earth System Model (CESM) [Lawrence et al. 2011]. With this coupling strategy, MEGAN v2.1 also uses the same vegetation dataset (i.e., 16 PFTs converted from the USGS dataset as discussed in Section 2.2) that CLM4 uses for all other land surface processes; this means, however, that MEGAN v2.1 can only be used with CLM4 in WRF-Chem. In addition, MEGAN v2.1 can compute BVOC emissions that account for the sub-grid variability of vegetation distributions within CLM4.

Chun Zhao 4/29/2016 10:40 AM
Deleted: mean values of

Chun Zhao 4/29/2016 10:40 AM
Deleted: days of

Chun Zhao 4/29/2016 10:40 AM
Deleted: temperature and solar radiation

Chun Zhao 4/29/2016 10:40 AM
Deleted: PFT's

2.4 Vegetation datasets

As mentioned previously, the first 16-PFT dataset (referred to as USGS hereafter)

used by CLM4 is converted from the default 24 USGS land cover dataset used by WRF-Chem based on a lookup table derived from Bonan et al. [1996]. This method is also applied to three other 16-PFTs datasets (referred to as VEG1, VEG2, and VEG3) used by CLM4 in WRF-Chem. The sensitivity of simulating BVOC emissions by CLM4 to these four 16-PFTs datasets is quantified. The VEG1, VEG2, and VEG3 datasets are derived from different sources as described next.

Chun Zhao 4/29/2016 10:40 AM
Deleted: PFT's

Chun Zhao 4/29/2016 10:40 AM
Deleted: PFT's

The VEG1 dataset is from the PFT fractional cover product by Ke et al. [2012], which was developed from the Moderate Resolution Imaging Spectroradiometer (MODIS) PFT classifications for the year 2005 for determining seven PFTs including needleleaf evergreen trees, needleleaf deciduous trees, broadleaf evergreen trees, broadleaf deciduous trees, shrub, grass and crop for each 500 m pixel. The WorldClim 5 arc-minute (0.0833°) [Hijmans et al., 2005] climatological global monthly surface air temperature and precipitation data was interpolated to a 500 m grid and used to further reclassify the PFTs into 15 PFTs, and fractions of crop grasses were mapped based on the method presented in Still et al. [2003]. Pixels with barren land and urban areas were reassigned to the bare soil class. The bare soil and the 15 PFTs from the 500-m grid were then aggregated to a 0.05° grid.

The VEG2 dataset is obtained from the NCAR CESM data repository [Oleson et al., 2010], available on a 0.05^{o} grid and derived using a combination of the 2001 MODIS Vegetation Continuous Field (VCF), MODIS land cover product for year 2000 [Lawrence and Chase, 2006; Lawrence and Chase, 2007], and 1992-1993 AVHRR Continuous Field Tree Cover Project data [Lawrence and Chase, 2007; Lawrence et al., 2011]. The monthly surface air temperature and precipitation data from Willmott and

277 Matsuura [2001] was used to further reclassify the seven PFTs into bare soil and 15 PFTs
278 in the tropical, temperate and boreal climate groups based on climate rules described by
279 Bonan et al. [2002]. Fractions of crop grasses were mapped based on the method
280 presented in Still et al. [2003].

281 The VEG3 dataset is derived from a high-resolution (30 arc-second) dataset over
282 the U.S. with 16 PFT classifications for the year 2008. The dataset was created by
283 combining the National Land Cover Dataset (NLCD, Homer et al., 2004) and the
284 Cropland Data Layer (see http://nassgeodata.gmu.edu/CropScape/), both of which were
285 based on the 30-m LANDSAT-TM satellite data. Vegetation species composition
286 information was obtained from the Forest Inventory and Analysis (see
287 http://www.fia.fs.fed.us) and the soil data from the Natural Resources Conservation
288 Services (see http://sdmdataaccess. nrcs.usda.gov/). The processing included adjusting
289 the NLCD tree cover estimates in urban areas to account for the substantial
290 underestimation of trees in the LANDSAT-TM data [Duhl et al., 2012]. This was
291 accomplished using the regionally specific adjustment factors for urban NLCD developed
292 by Greenfield et al. [2009] using the high-resolution imagery.

293 Figure 2 shows the spatial distributions of the dominant PFT in each 4×4 km^2 grid
294 cell of the simulation domain from each of the four datasets. Not only are the grid-
295 dominant PFTs very different among the four datasets, but the sub-grid distributions of
296 PFTs are different as well (not shown). The domain-averaged fractions of 16 PFTs from
297 the four datasets listed in Table 1 also illustrate the differences in PFT distributions. For
298 example, the fraction of temperate broadleaf deciduous tree ranges from 0.4% in VEG1
299 to 1.8% in VEG2 and the fraction of temperate broadleaf deciduous shrub ranges from

10.8% in VEG3 to 37.5% in VEG1. In MEGAN v2.0 of WRF-Chem, only four PFTs (refer to VEG-M) that are broadleaf tree, needleleaf tree, shrub, and herbaceous vegetation categories, are considered for the biogenic emission calculation because they are the only ones included in the MEGAN v2.0 PFT scheme. As discussed previously, these are different from the USGS vegetation distribution used by Noah and CLM4 and may cause additional biases. The distributions of the four PFTs used by MEGAN v2.0 are shown in Figure 3. This difference in PFT distributions can affect the BVOC emission calculations primarily through determining distributions of PFT specific emission factors and leaf area indices (LAI) that are prescribed with PFTs in this study. For example, Figure 4 shows the biogenic isoprene emission factor for each PFT prescribed in MEGAN v2.0 and MEGAN v2.1 in CLM4. In MEGAN v2.1, it shows that temperate broadleaf deciduous tree (PFT 7 listed in Table 1) has a large isoprene emission factor, while temperate needleleaf evergreen tree (PFT 1 listed in Table 1) has a small isoprene emission factor. A similar difference between broadleaf trees and needleleaf trees is indicated for MEGAN v2.0. Figure 5 shows the spatial distributions of averaged biogenic isoprene emission factor used in MEGAN v2.0 and v2.1 with different PFTs. It is evident that the difference in the distributions of PFTs results in a significant difference in spatial distributions of the isoprene emission factor. Figure 6 shows the spatial distributions of LAI used in MEGAN v2.0 and v2.1. The differences in the spatial distributions of LAI can significantly affect the biogenic emission calculation in MEGAN. It should be noted that in MEGAN v2.0 used in WRF-Chem, the LAI used for the calculation of the biogenic emissions is prescribed using the 4 PFTs, which is different than the land scheme that uses the LAI derived from the 24 USGS land categories.

Chun Zhao 4/29/2016 10:40 AM
Moved (insertion) [1]

Chun Zhao 4/29/2016 10:40 AM
Deleted: .

Chun Zhao 4/29/2016 10:40 AM
Deleted: 3

Chun Zhao 4/29/2016 10:40 AM
Deleted: It

Chun Zhao 4/29/2016 10:40 AM
Deleted: Finally, the distribution of

Chun Zhao 4/29/2016 10:40 AM
Deleted: tree,

Chun Zhao 4/29/2016 10:40 AM
Deleted: tree, shrub, and herbaceous vegetation categories used by MEGAN v2.0 (refer to VEG-M)

Chun Zhao 4/29/2016 10:40 AM
Deleted: shown in Figure 4. In MEGAN v2.0 of WRF-Chem, only these four PFT's are considered for the biogenic emission calculation because they are the only ones included in the MEGAN v2.0 PFT scheme.

Chun Zhao 4/29/2016 10:40 AM
Moved up [1]: As discussed previously, these are different from the USGS vegetation distribution used by Noah and CLM4 and may cause additional biases.

2.5 Numerical experiments

The simulations are performed using a domain encompassing California (Fig. 1) with a horizontal grid spacing of 4 km and 279×279 grid cells (113°W-128°W, 32°N-43°N) and 51 vertical layers up to 100 hPa with about 35 layers below 2 km. The simulation period is from May 25 to June 30 2010, but only the results in June are used for analysis to allow for the model to "spin-up" realistic distributions of trace gases. The initial and boundary conditions are prescribed by large-scale meteorological fields obtained from the North American Regional Reanalysis (NARR) data with updates provided at 6-h intervals, which also provide the prescribed sea surface temperature (SST) for the simulations. The modeled u and v wind components and temperature in the free atmosphere above the planetary boundary layer are nudged towards the NARR reanalysis data with a time scale of 6 hours [Stauffer and Seaman, 1990]. Chemical lateral boundary conditions are from the default profiles in WRF-Chem, which are based on the averages of mid-latitude aircraft profiles from several field studies over the eastern Pacific Ocean [McKeen et al., 2002].

Chun Zhao 4/29/2016 10:40 AM
Deleted: -component

Chun Zhao 4/29/2016 10:40 AM
Deleted: -component

Chun Zhao 4/29/2016 10:40 AM
Deleted: atmospheric

Chun Zhao 4/29/2016 10:40 AM
Deleted: nudging

Anthropogenic emissions were obtained from the CARB 2008 ARCTAS emission inventory developed for the NASA Arctic Research of the Composition of the Troposphere from Aircraft and Satellite (ARCTAS) mission over California [Pfister et al., 2011]. The CARB inventory contains hourly emissions for a 13-day period using a 4-km grid spacing over California. We created diurnally averaged emissions from 5 of the weekdays and 2 of the weekend days and used those averages for all weekdays and weekends and applied these over the entire simulation period. Anthropogenic emissions

367 from the 2005 National Emissions Inventory (NEI) (WRF-Chem user guide from
368 http://ruc.noaa.gov/wrf/WG11/Users guide.pdf) were used for regions outside of
369 California. Biomass burning is not considered in the present study, because satellite
370 detection methods indicated that there were very few fires in California during the
371 simulation period. Biogenic emissions were computed on-line using the MEGAN model
372 and lumped into isoprene, terpenes, and sesquiterpenes for the SAPRC-99 photochemical
373 mechanism.

374 As discussed previously, multiple numerical experiments summarized in Table 2
375 are conducted with different combinations of land surface schemes and vegetation
376 datasets to investigate the sensitivity of BVOC simulation to land surface schemes and
377 vegetation distributions. First, we conduct two experiments using MEGAN v2.0 coupled
378 with the Noah (Mv20Noah) and CLM4 (Mv20CLM) land surface schemes, respectively.
379 The Noah land surface scheme is only coupled with MEGAN v2.0 in WRF-Chem. In
380 these two experiments, the two land surface schemes use the USGS vegetation
381 distributions while MEGAN v2.0 uses a separate vegetation map (VEG-M) to estimate
382 BVOC emissions. By comparing these two experiments, the impact of land surface
383 schemes on simulated BVOC concentrations are examined. Second, we conduct four
384 experiments using MEGAN v2.1 embedded in the CLM4 land surface scheme with four
385 different vegetation datasets, i.e., USGS (Mv21USGS), VEG1 (Mv21V1), VEG2
386 (Mv21V2), and VEG3 (Mv21V3). The differences among these four experiments show
387 the impact of vegetation distributions on simulated BVOC concentrations.

388 We note that MEGAN v2.0 and v2.1 use different vegetation datasets and are
389 implemented in WRF-Chem in different ways, but the objective of this study is not to

Chun Zhao 4/29/2016 10:40 AM
Deleted: BVOCs

Chun Zhao 4/29/2016 10:40 AM
Deleted: BVOCs

392 explore how the formulations of these two versions of MEGAN affect BVOC
393 concentrations. The better way for exploring the version difference of MEGAN is to
394 implement both versions in the same way and use the same vegetation dataset. The
395 simulated BVOC emissions and concentrations by WRF-Chem with MEGAN v2.0 and
396 MEGAN v2.1 are included together here as a reference for future studies in the
397 community and for users interested in migrating from the widely used v2.0 to v2.1.
398
399 **3. Observations**
400 Measurements of VOCs collected by proton transfer reaction mass spectrometer
401 (PTR-MS) instruments [Lindinger et al., 1998] and a gas chromatography instrument
402 [Gentner et al., 2012] over California during June of 2010 as part of the CARES and
403 CalNex campaigns are used to evaluate the simulated isoprene and monoterpene
404 concentrations. CARES was designed to address science issues associated with the
405 interactions of biogenic and anthropogenic precursors on SOA, black carbon mixing state,
406 and the effects of organic species and aerosol mixing state on optical properties and the
407 activation of cloud condensation nuclei [Zaveri et al., 2012]. As shown in Figure 7,
408 ground-based instruments were deployed at two sites (T0 and T1) in northern California:
409 T0 in Sacramento (38.649 °N, -121.349°W, ~ 30 m m.s.l., denoted by red upward
410 triangle) and T1 in Cool (38.889°N, -120.974°W, ~ 450 m m.s.l., denoted by red
411 downward triangle), a small town located about 40 km northeast of Sacramento. The U.S.
412 Department of Energy (DOE) Gulfstream 1 (G-1) research aircraft sampled
413 meteorological, trace gas, and aerosol quantities aloft in the vicinity of the T0 and T1
414 sites, denoted by black lines in Figure 8. Zaveri et al. [2012] described the

Chun Zhao 4/29/2016 10:40 AM
Deleted: 5

Chun Zhao 4/29/2016 10:40 AM
Deleted: 6

instrumentation for each of the surface sites and Shilling et al. [2013] described VOC measurements on the G-1. Most of the sampling during CARES occurred between 2 and 28 June, and only the aircraft sampling within 1 km of the surface is used to evaluate model simulations because G-1 sampled below 1 km for the majority of time.

CalNex was designed to address science issues relevant to emission inventories, dispersion of trace gases and aerosols, atmospheric chemistry, and the interactions of aerosols, clouds, and radiation [Ryerson et al., 2013]. Ground-based instruments were deployed at two sites in southern California as shown in Figure 7: one in Pasadena (34.141°N, -118.112°W, ~240 m m.s.l., denoted by the red circle) and one in Bakersfield (35.346°N, −118.965°W, ~ 123 m m.s.l., denoted by the red square). The NOAA WP-3D research aircraft sampled meteorological, trace gas, and aerosol quantities aloft along flight paths shown in Figure 7 (denoted by blue lines). While most of the CalNex aircraft tracks below an altitude of 1 km were conducted in southern California in the vicinity of the Los Angeles basin, the WP-3D also flew within the Central Valley and in the vicinity of Sacramento on some days. A detailed description of the instrumentation for each of the CalNex surface sites and mobile platforms is given by Ryerson et al. [2013]. Most of the sampling during CalNex was conducted before June 16 and only the aircraft sampling below 1 km is used to evaluate the model simulations.

Chun Zhao 4/29/2016 10:40 AM
Deleted: 5

Chun Zhao 4/29/2016 10:40 AM
Deleted: 5

4. Results

4.1 Impact of land surface schemes

4.1.1 Biogenic isoprene and monoterpene emissions

Figure 7 shows the spatial distributions of biogenic isoprene emissions averaged

Chun Zhao 4/29/2016 10:40 AM
Deleted: 5

over June for the six simulations listed in Table 2. Biogenic isoprene emissions occur in vegetated regions of California with the highest emission rates along the foothills of the Sierra Nevada where oak trees are the dominant plant species. To show the difference in biogenic isoprene emissions among the cases more clearly, Figure 8a and 8b zoom in on the CARES (northern California) and CalNex (southern California) sampling regions, respectively. In both regions the differences in land surface schemes had a relatively small impact on the biogenic isoprene emissions over California in terms of both spatial distribution and magnitude, although the emissions from Mv20CLM were a little larger than those from Mv20Noah. The domain summed biogenic isoprene emissions for the entire month of June from Mv20Noah and Mv20CLM are 1.4×10^{9} and 1.6×10^{9} mole, respectively. Figure 9a and 9b are similar to Figure 8a and 8b, except that biogenic monoterpene emission fluxes are shown. In general, the spatial patterns of emissions of the two biogenic species are similar, except that the peak areas of monoterpene emissions are shifted slightly. For example, the peak monoterpene emissions in northern California occur further northeast at higher elevations of the Sierra Nevada that are dominated by needleleaf evergreen trees. The impact of land surface schemes on biogenic monoterpene emissions is also small over California in terms of both spatial patterns and magnitudes, although the emissions from Mv20CLM are a little larger than those from Mv20Noah. The domain summed biogenic monoterpene emissions for the entire month of June from Mv20Noah and Mv20CLM are $1.0\text{x}10^{8}$ and $1.1\text{x}10^{8}$ mole, respectively.

The similarity in estimating biogenic emissions between the experiments with two land surface schemes is also summarized in Figures 10 and 11, which show the average diurnal biogenic isoprene and monoterpene emission rates at the four observation sites.

Chun Zhao 4/29/2016 10:40 AM
Deleted: 6a

Chun Zhao 4/29/2016 10:40 AM
Deleted: 6b

Chun Zhao 4/29/2016 10:40 AM
Deleted: 7a

Chun Zhao 4/29/2016 10:40 AM
Deleted: 7b

Chun Zhao 4/29/2016 10:40 AM
Deleted: 6a

Chun Zhao 4/29/2016 10:40 AM
Deleted: 6b

Chun Zhao 4/29/2016 10:40 AM
Deleted: 8

Chun Zhao 4/29/2016 10:40 AM
Deleted: 9

Chun Zhao 4/29/2016 10:40 AM
Deleted: monterpene

The similarity between Mv20Noah and Mv20CLM (red and orange lines) is likely due to the same vegetation map in MEGAN v2.0 to estimate biogenic emissions. Although the two land surface schemes produce slightly different values of surface temperature (Fig. 1), soil moisture (not shown), and net solar radiation near the surface (not shown), their impact on the biogenic emissions was small. Both BVOC species have peak emission rates in the early afternoon. One noteworthy difference in diurnal variation of the two biogenic species emission rates is that there is no isoprene emitted during the night while the amount of monoterpenes emitted during the night is small but not negligible. This can contribute to differences in the diurnal variation of the mixing ratios of two biogenic species, as will be discussed next.

4.1.2 Isoprene and monoterpene mixing ratios

Figures 12a,b and 13a,b show the spatial distributions of monthly-averaged surface mixing ratios of isoprene+MVK(methyl-vinylketone)+MACR(methacrolein) and monoterpenes, respectively, around the CARES (northern California) and the CalNex (central and southern California) sampling regions simulated by the six experiments listed in Table 2. Due to the fast chemical transition from isoprene to MVK and MACR, the sum of isoprene+MVK+MACR mixing ratios can better reflect the impact of biogenic isoprene emissions than isoprene mixing ratio alone [Shilling et al., 2013]. In general, the spatial patterns and magnitudes of surface isoprene+MVK+MACR and monoterpene mixing ratios over the two regions are similar from the two MEGAN v2.0 experiments with the Noah and CLM4 land surface schemes, respectively. The spatial patterns of surface mixing ratios of isoprene+MVK+MACR and monoterpenes are similar to the spatial variability in the emission rates.

Chun Zhao 4/29/2016 10:40 AM
Deleted: some difference in

Chun Zhao 4/29/2016 10:40 AM
Deleted: 10a

Chun Zhao 4/29/2016 10:40 AM
Deleted: 11a

Chun Zhao 4/29/2016 10:40 AM
Deleted: monoterpene

There is difference between the two experiments at specific locations, which is partly reflected in the comparison of average diurnal variations of surface mixing ratios of isoprene+MVK+MACR and monoterpenes at the four observation sites shown in Figure 14 and Figure 15. At the Bakersfield site, only isoprene mixing ratios were reported so that the comparison is for isoprene only. Note that the values for the Bakersfield and Pasadena sites are averaged over the first two weeks of June to be consistent with the observations. Although both experiments with Noah and CLM4 (red and orange lines, respectively) simulate similar isoprene emission fluxes with the maximum in the afternoon (Fig. 10), their respective isoprene+MVK+MACR mixing ratios are different at the four sites, particularly at site T0, where the Mv20CLM simulated isoprene+MVK+MACR mixing ratios during the daytime are about a factor of 2 larger than those from Mv20Noah. This inconsistence mainly results from the differences in the near surface meteorology, such as net surface radiation and temperature, between the two experiments (not shown) that affects photochemistry, but this impact of surface meteorology occurs only at limited locations. When compared to the observations, both experiments significantly underestimate the isoprene+MVK+MACR mixing ratios except at the Bakersfield site. Figure 15 is identical to Figure 14, except for surface monoterpene mixing ratios. Note that there were no monoterpene data reported for the Bakersfield and Pasadena sites, so only the simulation results are shown. In contrast to isoprene+MVK+MACR, monoterpenes exhibit peak surface mixing ratios during the nighttime due to the strong photolysis activity that makes the lifetime of monoterpenes short during the daytime and the small emissions into a shallow boundary layer during the nighttime (Fig. 11). In general, the

Chun Zhao 4/29/2016 10:40 AM
Deleted: monoterpene

Chun Zhao 4/29/2016 10:40 AM
Deleted: 12

Chun Zhao 4/29/2016 10:40 AM
Deleted: 8

Chun Zhao 4/29/2016 10:40 AM
Deleted: the

Chun Zhao 4/29/2016 10:40 AM
Deleted: difference

Chun Zhao 4/29/2016 10:40 AM
Deleted: difference

Chun Zhao 4/29/2016 10:40 AM
Deleted: .

Chun Zhao 4/29/2016 10:40 AM
Deleted: 13

Chun Zhao 4/29/2016 10:40 AM
Deleted: 12

Chun Zhao 4/29/2016 10:40 AM
Deleted: 9

difference between the Mv20Noah and MV20CLM experiments in monoterpene mixing ratios is relatively small at these four sites, particularly during the daytime. When compared to the observations, both experiments overestimate the diurnal variation and the nighttime surface monoterpene mixing ratios at the T0 and T1 sites.

Figures 16 and 17 show the comparison of the observed and simulated mixing ratios of isoprene+MVK+MACR and monoterpenes, respectively, along the G-1 and WP-3D flight tracks below 1 km. Model results are sampled along the flight tracks. As shown in Figure 7, the G-1 flight mainly flew over northern California around the T0 and T1 sites, while the WP-3D flew over a larger area covering both southern California and the Central Valley. To better reflect the spatial variability in the BVOCs, the flight tracks of both flights are separated into two regions as indicated by the black lines in Figure 12a,b and Figure 13a,b. For the G-1, the flight paths are divided into regions of southwest and northeast of the black line shown in Figures 12a and 13a that is parallel to the Sierra Nevada. The two regions have significantly different vegetation (Fig. 2) resulting in large differences in biogenic emissions. For the WP-3D, the flight paths are divided into regions of south and north of the black line shown in Figures 12b and 13b to separate southern California and the Central Valley. Over southern California, the measured isoprene+MVK+MACR mixing ratios by the PTR-MS over the WP-3D are the upper limit since the PTR-MS may have a small interference in urban areas for isoprene and MVK+MACR.

In Figure 16, it is interesting to note that both experiments Mv20Noah and Mv20CLM reasonably capture the variability seen in the G-1 isoprene+MVK+MACR measurements over the southwest region even though they underestimate the surface

Chun Zhao 4/29/2016 10:40 AM
Deleted: 14

Chun Zhao 4/29/2016 10:40 AM
Deleted: 15

Chun Zhao 4/29/2016 10:40 AM
Deleted: monoterpene

Chun Zhao 4/29/2016 10:40 AM
Deleted: 5

Chun Zhao 4/29/2016 10:40 AM
Deleted: 10a

Chun Zhao 4/29/2016 10:40 AM
Deleted: 11a

Chun Zhao 4/29/2016 10:40 AM
Deleted: 10a

Chun Zhao 4/29/2016 10:40 AM
Deleted: 11a

Chun Zhao 4/29/2016 10:40 AM
Deleted: 10b

Chun Zhao 4/29/2016 10:40 AM
Deleted: 11b

Chun Zhao 4/29/2016 10:40 AM
Deleted: 14

observations by as much as a factor of 2 at the T0 site (Fig. 14). While both experiment mixing ratios are slightly smaller than observed, the Mv20CLM simulated mixing ratios are a little larger than those from Mv20Noah and closer to the observations. Over the northeast region, both experiments produced similar mixing ratios that were significantly smaller than the observations, which is consistent with the comparison between the simulated and observed isoprene+MVK+MACR at the T1 site (Fig. 14). As shown in Figure 16, the Mv20CLM simulation produced somewhat larger isoprene+MVK+MACR mixing ratios than Mv20Noah in both southern California and the Central Valley. This is consistent with the comparison at the Bakersfield and Pasadena surface sites. Both simulations also underestimate and overestimate the isoprene+MVK+MACR mixing ratios over southern California and the Central Valley, respectively. The comparison of isoprene+MVK+MACR with aircraft observations may suggest that both experiments underestimate biogenic isoprene emissions over the forested foothills of Sierra Nevada and southern California around Los Angeles, but overestimate the emissions over the Central Valley. The model biases may also be affected, to some extent, by anthropogenic emissions with large uncertainties and the associated non-linear chemistry due to the mixing of anthropogenic and biogenic plumes [Fast et al., 2014].

Figure 17 shows that both experiments Mv20Noah and Mv20CLM significantly underestimate the monoterpene mixing ratios over all the regions sampled by the G-1 and WP-3D aircraft and that the differences between the simulations were negligible. The average monoterpene mixing ratios sampled by the G-1 below 1 km was comparable to the surface measurement at the T0 site during the daytime, but somewhat higher than the observations at the T1 site. The simulated mixing ratios averaged along the flight tracks

Chun Zhao 4/29/2016 10:40 AM
Deleted: 12

Chun Zhao 4/29/2016 10:40 AM
Deleted: experiments

Chun Zhao 4/29/2016 10:40 AM
Deleted: 12

Chun Zhao 4/29/2016 10:40 AM
Deleted: 14

Chun Zhao 4/29/2016 10:40 AM
Deleted: 15

were much smaller than those at the two surface sites, suggesting that it may be difficult for model to simulate the large spatial heterogeneity of the monoterpene mixing ratios. This could result from the biases in biogenic monoterpene emissions and/or the chemical mechanism for monoterpene oxidation and how chemistry is coupled with turbulent mixing within the simulated convective boundary layer. It also needs to be noted that the G-1 and WP-3D measured monoterpene mixing ratios are generally below the Limit Of Detection (LOD) of instruments (0.1-0.3 ppbv). Therefore, the true monoterpene mixing ratios could be range between 0 ~ 0.1-0.3 ppbv, which may also contribute to the discrepancy between observations and simulations.

4.2 Impact of vegetation distributions

4.2.1 Biogenic isoprene and monoterpene emissions

Figures 8a,b and 9a,b show that the differences in biogenic isoprene and monoterpene emission distributions due to using the various vegetation datasets are larger than the differences resulting from the two land surface schemes. The domain summed biogenic isoprene emissions for the entire month of June are 2.3, 0.76, 1.7, and 0.92 ($\times 10^9$ mole) from the experiments of Mv21USGS, Mv21V1, Mv21V2, and Mv21V3, respectively, and biogenic monoterpene emissions are 2.5, 1.7, 1.9, and 1.1 ($\times 10^8$ mole) from the four experiments, respectively. Each of the four simulations produces high biogenic isoprene and monoterpene emission rates along the Sierra Nevada that is covered mainly by oak and pine forests. However, the different forest classifications and their coverage (Table 1) produce different biogenic isoprene and monoterpene emission rates along the Sierra Nevada. Another distinct difference among these four simulations

Chun Zhao 4/29/2016 10:40 AM
Deleted: 6a

Chun Zhao 4/29/2016 10:40 AM
Deleted: 7a

is found over the Central Valley, where the Mv21V1 and Mv21V3 experiments produce significantly lower biogenic isoprene and monoterpene emissions than the Mv21USGS and Mv21V2 experiments. This results from their different spatial distributions of vegetation types. For example, the vegetation dataset in MV21USGS assigns a relatively larger fraction of vegetation over the Central Valley to broadleaf trees, which are biggest contributors of isoprene emissions (Fig. 4).

The differences in the spatial distributions of biogenic isoprene and monoterpene emissions due to various vegetation distributions is also illustrated by the average diurnal biogenic isoprene emission rates at the four observation sites shown in Figures 10 and 11. For example, the Mv21V3 simulation produces the largest biogenic isoprene and monoterpene emissions at three of the sites. At the T1 site over the forested foothills of the Sierra Nevada, the Mv21USGS and Mv21V3 simulations produce much larger biogenic isoprene emissions than Mv21V1 and Mv21V2. Even though forest is the dominant vegetation type along the foothills of the Sierra Nevada in all four vegetation datasets (Fig. 2), their different forest classifications and coverage result in biogenic isoprene emission rates that differ by as much as a factor of 8 at the T1 site. Similar to isoprene emissions, the Mv21USGS simulation produces the largest monoterpene emissions at the T1 site. However, the differences in monoterpene emissions among the four vegetation dataset experiments are smaller overall than that for biogenic isoprene emissions. Different vegetation distributions for a typical urban area can also lead to differences in biogenic isoprene and monoterpene emissions. For example at the urban T0 and Pasadena sites, biogenic isoprene and monoterpene emission rates are almost 0 in the Mv21USGS and Mv21V1 experiments, while the rates were significant larger in the

Chun Zhao 4/29/2016 10:40 AM
Deleted: 3

Chun Zhao 4/29/2016 10:40 AM
Deleted: 8

Chun Zhao 4/29/2016 10:40 AM
Deleted: 9

Mv21V3 experiment. This could have profound implications on local oxidant chemistry influencing urban air quality.

4.2.2 Isoprene+MVK+MACR and monoterpene mixing ratios

As expected, the differences in biogenic isoprene and monoterpene emissions among the four different vegetation distribution experiments lead to large differences in the simulated surface isoprene+MVK+MACR and monoterpene mixing ratios (Figs. 12a,b and 13a,b). Although all the four experiments simulate highest biogenic isoprene+MVK+MACR and monoterpene mixing ratios along the forested foothills of Sierra Nevada, the Mv21V1 and Mv21V3 experiments have the lowest isoprene+MVK+MACR and monoterpene mixing ratios, respectively, corresponding to their lowest biogenic emission rates. Over the Central Valley, Mv21USGS and Mv21V2 experiments produce significantly higher isoprene+MVK+MACR mixing ratios than the other two experiments, while Mv21V3 simulates the lowest monoterpene mixing ratios among all the experiments.

At the T1 site located in the forested foothills of Sierra Nevada, the Mv21V1 simulation produces the lowest isoprene+MVK+MACR mixing ratios (Fig. 14), significantly underestimating the peak concentrations during the day. In contrast, the Mv21USGS and Mv21V3 simulations reasonably capture the observed isoprene+MVK+MACR mixing ratios during the daytime. All four experiments underestimate the isoprene+MVK+MACR mixing ratios by about a factor of 2 during the night. This may indicate that the transported isoprene+MVK+MACR from the surrounding areas of T1 was too low. The negative biases of simulated isoprene+MVK+MACR mixing ratios over the areas surrounding T1 can be reflected by

Chun Zhao 4/29/2016 10:40 AM
Deleted: 10a

Chun Zhao 4/29/2016 10:40 AM
Deleted: 11a

Chun Zhao 4/29/2016 10:40 AM
Deleted: 12

Figure 16 that shows all the four experiments significantly underestimate the observed isoprene+MVK+MACR mixing ratios below 1 km in the northeast area around the T1 site (Fig. 12a). Figure 16 also shows that Mv21USGS and MV21V3 simulate larger isoprene+MVK+MACR mixing ratios averaged over the northeast region of northern California than Mv21V1 and Mv21V2. All four experiments produce similar surface monoterpene mixing ratios, which are smaller than that from the Mv20Noah and Mv20CLM with MEGAN v2.0 and are closer to the observed values particularly during the night. This is consistent with their much lower biogenic monoterpene emissions during the night (Fig. 11). The four experiments with MEGAN v2.1 simulate higher daytime monoterpene mixing ratios averaged along the flight tracks below 1 km than the two experiments with MEGAN v2.0. The simulated mixing ratios are still much lower than the aircraft observations, although the simulated surface mixing ratios are higher than the observations at the T1 site (Fig. 15). However, the aircraft measured monoterpene mixing ratios may also be higher than the true values due to the LOD of instruments (0.1-0.3 ppbv).

At the T0 site, an urban site, the vegetation coverage in both the Mv21USGS and Mv21V1 experiments is small so that the isoprene+MVK+MACR and monoterpene mixing ratios are significantly lower than observed during the daytime. The Mv21V2 and Mv21V3 experiments reasonably simulate isoprene+MVK+MACR mixing ratios during the daytime. Over the area surrounding the T0 site (i.e., the southwest area in Fig. 12a), it is interesting to note that the Mv21USGS and Mv21V2 simulations produced larger isoprene+MVK+MACR mixing ratios than Mv21V1 and Mv21V3 and closer to the observations (Fig. 16). This is mainly due to the relatively large isoprene+MVK+MACR

Chun Zhao 4/29/2016 10:40 AM
Deleted: 14

Chun Zhao 4/29/2016 10:40 AM
Deleted: 10a

Chun Zhao 4/29/2016 10:40 AM
Deleted: 14

Chun Zhao 4/29/2016 10:40 AM
Deleted: v20

Chun Zhao 4/29/2016 10:40 AM
Deleted: 9

Chun Zhao 4/29/2016 10:40 AM
Deleted: v21

Chun Zhao 4/29/2016 10:40 AM
Deleted: v20

Chun Zhao 4/29/2016 10:40 AM
Deleted: 13

Chun Zhao 4/29/2016 10:40 AM
Deleted: 10a

Chun Zhao 4/29/2016 10:40 AM
Deleted: 14

mixing ratios over the northwest corner of CARES sampling region (Fig. 12a) in the Mv21USGS and Mv21V2 simulations, consistent with the distributions of biogenic isoprene emissions over the region. The Mv21V2 and Mv21V3 simulations produced higher monoterpene mixing ratios than Mv21USGS and Mv21V1, but are still smaller than the observed values during the daytime not only for the T0 site but also for the region surrounding T0 as shown in Figure 17.

At the Bakersfield site, the experiments often simulate significantly larger isoprene mixing ratios than the observations, except for the Mv21V1 simulation that was always too small. The Mv21V3 simulation produced the highest isoprene mixing ratios among the experiments. This is consistent with its biogenic isoprene emission rates (Fig. 10). In addition, the observed surface isoprene mixing ratios show negligible diurnal variation in contrast to the experiments that produced larger diurnal variations. The Mv21V3 simulation produced peak isoprene mixing ratios during the daytime that were likely controlled by its large daytime local biogenic isoprene emission rates (Fig. 10). The Mv21USGS and Mv21V2 simulations produced peak isoprene mixing ratios during the early evening, possibly the result of chemistry and transport from regions with higher biogenic emissions. All four experiments produce small diurnal variation of surface monoterpene mixing ratios. The Mv21USGS and Mv21V3 simulations produce larger monoterpene mixing ratios than the other two, consistent with their local emission rates (Fig. 11).

At the Pasadena site, the Mv21V3 simulation reproduces the observed diurnal variation of isoprene+MVK+MACR mixing ratios reasonably well. This is consistent with the area surrounding the Pasadena site, in which the Mv21V3 simulation produces

Chun Zhao 4/29/2016 10:40 AM
Deleted: 10a

Chun Zhao 4/29/2016 10:40 AM
Deleted: 15

Chun Zhao 4/29/2016 10:40 AM
Deleted: only isoprene mixing ratios were reported. The

Chun Zhao 4/29/2016 10:40 AM
Deleted: 8

Chun Zhao 4/29/2016 10:40 AM
Deleted: 8

Chun Zhao 4/29/2016 10:40 AM
Deleted: 9

the largest mixing ratios of isoprene+MVK+MACR both at the surface (Fig. 12b) and aloft (Fig. 16) in the vicinity of Los Angeles. The other three experiments simulated significantly smaller mixing ratios of isoprene+MVK+MACR. Although the values from the other three experiments are still smaller than the observations, they are much closer to the aircraft measurements (within a factor of 2) than at the Pasadena site (Fig. 14). Among the four vegetation sensitivity simulations, Mv21V3 produces higher surface monoterpene mixing ratios than the other three experiments, consistent with their emission rates (Fig. 11). All four vegetation sensitivity experiments produced much lower monoterpene mixing ratios below 1 km (Fig. 17), compared to the aircraft measurements over southern California that may overestimate the true values due to the LOD of instruments (0.1-0.3 ppbv).

As discussed previously, all four experiments simulate significantly different isoprene+MVK+MACR and monoterpene mixing ratios over the Central Valley (Figs. 12a,b and 13a,b). The Mv21USGS and Mv21V2 simulations produce much larger isoprene+MVK+MACR mixing ratios (0.6 ppbV and 0.5 ppbV, respectively) over the Central Valley than the observed values (~0.1 ppbV). The Mv21V1 and Mv21V3 simulations produce monoterpene mixing ratios much closer to observed values. This may indicate that the fraction of broadleaf trees (the main emitter over the region) over the Central Valley from the vegetation datasets USGS and VEG2 are overestimated or the biogenic emission factors estimated for the broadleaf trees are overestimated for this area. For monoterpenes, the Mv21V3 simulation was much smaller than observed, while the mixing ratios from the other three experiments were more comparable. This suggests that the fraction of vegetation emitting monoterpenes is significantly underestimated over

Chun Zhao 4/29/2016 10:40 AM
Deleted: 10b

Chun Zhao 4/29/2016 10:40 AM
Deleted: 14

Chun Zhao 4/29/2016 10:40 AM
Deleted: 12

Chun Zhao 4/29/2016 10:40 AM
Deleted: 9

Chun Zhao 4/29/2016 10:40 AM
Deleted: 15

Chun Zhao 4/29/2016 10:40 AM
Deleted: 10a

Chun Zhao 4/29/2016 10:40 AM
Deleted: 11a

767 this area in the VEG3 dataset.

768

769 **5. Summary and discussion**

770 In this study, the latest version of MEGAN (v2.1) is coupled within the CLM4
771 land scheme as part of WRF-Chem. Specifically, MEGAN v2.1 is implemented into the
772 CLM4 scheme so that a consistent vegetation map can be used for estimating biogenic
773 VOC emissions as well as surface fluxes. This is unlike the older version of MEGAN
774 (v2.0) in the public-released WRF-Chem that uses a standalone vegetation map that
775 differs from what is used in land surface schemes. With this improved WRF-Chem
776 modeling framework coupled with CLM4-MEGAN v2.1, the sensitivity of biogenic VOC
777 emissions and hence of atmospheric VOC mixing ratios to vegetation distributions is
778 investigated. The WRF-Chem simulations are also conducted with the two land surface
779 schemes, Noah and CLM4, with the MEGAN v2.0 scheme for biogenic emissions in each
780 case. The comparison between the Noah and CLM4 driven MEGAN v2.0 biogenic
781 emissions not only serves for investigating the impact of different land surface schemes
782 on the emissions but also provides a reference for all previous studies that used the Noah
783 land surface scheme. Experiments are conducted for June 2010 over California,
784 compared with the measurements from the CARES and CalNex campaigns. The main
785 findings about the modeling sensitivity to the land surface schemes and vegetation
786 distributions include:

787 • The WRF-Chem simulation with the CLM4 land surface scheme and the MEGAN
788 v2.0 module (Mv20CLM) produces similar biogenic isoprene and monoterpene
789 emissions in terms of spatial patterns, magnitudes, and diurnal variations as the one

Chun Zhao 4/29/2016 10:40 AM
Deleted: the

with the Noah land surface scheme (Mv20Noah) in June over California. The similarity in the biogenic emissions between the experiments using two different land schemes is primarily because of using MEGAN v2.0 and the same vegetation map in the two experiments. The spatial patterns and magnitudes of surface isoprene+MVK+MACR and monoterpene mixing ratios are generally similar between the two experiments with the Noah and CLM4 land surface schemes, although there are significant differences at some specific locations due to their differences in the near surface meteorology such as surface net radiation and temperature. Compared with surface and aircraft measurements, both experiments generally underestimate the daytime mixing ratios of isoprene+MVK+MACR but overestimate the nighttime mixing ratios of monoterpenes.

- The experiments with the four vegetation datasets result in much larger differences in biogenic isoprene and monoterpene emissions than the ones with the two land surface schemes. The simulated total biogenic isoprene and monoterpene emissions over California can differ by a factor of 3 among the experiments and the difference can be even larger over specific locations. The comparison of mixing ratios of isoprene+MVK+MACR and monoterpenes with the observations indicates the simulation biases can be largely reduced with accurate vegetation distributions over some regions of California. For example, at an observation site at the forested foothills of Sierra Nevada, two experiments with the vegetation distributions from the USGS and VEG3 datasets capture the observed daytime surface mixing ratios of isoprene+MVK+MACR well, with values that are much larger than the experiments with the other two vegetation datasets.

- Although vegetation distributions from some datasets do significantly improve the model performance in simulating BVOC mixing ratios more than others, the optimal vegetation dataset cannot be determined, because the improvement by vegetation datasets has dependence on both the region and BVOC species of interest. For example, over the Central Valley, the experiments with the VEG1 and VEG3 vegetation datasets simulate isoprene+MVK+MACR mixing ratios that are much closer to observations than the USGS and VEG2 datasets, while the VEG3 dataset significantly underestimates the observed monoterpene mixing ratios. Large biases over some regions of California in all the experiments with current vegetation datasets imply that more effort is needed to improve land cover datasets and/or biogenic emission factors.

There are still some large biases existing over some regions of California regardless of the vegetation distributions. For example, all the experiments significantly underestimate the observed isoprene+MVK+MACR mixing ratios below an altitude of 1 km over the forest-covered Sierra Nevada. Over the Pasadena area, all the experiments simulate significantly smaller monoterpene mixing ratios than observed. The biases in BVOCs identified in this study may be partly due to inaccurate vegetation distributions in all the vegetation distribution datasets. The biases can also result from the uncertainties in BVOC emission factors for the individual types of vegetation commonly found in California. The constraints on BVOC emission factors applied in models are limited due to sparse measurements of BVOC emission fluxes. The MEGAN scheme in WRF-Chem uses the global averaged emission factors for BVOC emissions for each PFT. Over California, the broadleaf temperate trees are primarily oaks that have relatively higher

Chun Zhao 4/29/2016 10:40 AM
Deleted: BVOCs

Chun Zhao 4/29/2016 10:40 AM
Deleted: BVOCs

Chun Zhao 4/29/2016 10:40 AM
Deleted: BVOCs

Chun Zhao 4/29/2016 10:40 AM
Deleted: BVOCs

BVOC emission factors compared to the global mean values for temperate broadleaf trees. In addition, the needleleaf trees are pines that have relatively larger monoterpene emission factors compared to global mean values. These biases in emission factors may partly explain why all the experiments generally underestimate mixing ratios of isoprene+MVK+MACR and monoterpenes over the regions with large amounts of trees. The MEGAN scheme using the location-specified emission factor maps that accounts for species composition of trees may provide a better estimate on regional scales.

This study demonstrates large difference between the experiments with the two versions of MEGAN (v2.0 versus v2.1), and that MEGAN v2.1 results in a better comparison with the observations over some parts of the study domain. However, this difference should not be fully attributed to the improvement of MEGAN between the two versions, because the two versions also use different vegetation distributions. The results highlight the importance of sub-grid vegetation distributions in simulating biogenic emissions even at a relatively high horizontal grid spacing (e.g., 4 km in this study). The biogenic emissions can be significantly different even though the dominant vegetation within a model grid box is similar. The comparison of the simulations and the observations at the surface sites and along the aircraft tracks reflects the large spatial variability of biogenic emissions and BVOC mixing ratios over California. It is challenging for model to capture such a spatial heterogeneity of BVOCs if the vegetation distributions are not appropriately represented in the simulation. The relatively large LOD of instruments on the aircrafts for monoterpenes compared to the true concentrations also make the evaluation of simulated monoterpenes difficult. Over a region with relatively low monoterpene concentrations, an instrument with lower LOD is

Chun Zhao 4/29/2016 10:40 AM
Deleted: BVOCs

Chun Zhao 4/29/2016 10:40 AM
Deleted: v20

Chun Zhao 4/29/2016 10:40 AM
Deleted: v21

Chun Zhao 4/29/2016 10:40 AM
Deleted: v21

Chun Zhao 4/29/2016 10:40 AM
Deleted: BVOCs

needed. It is also noteworthy that this study is in a relatively dry and warm season; therefore the impact of biogenic emission treatments may change for other seasons and during periods with higher cloudiness. A multiple-season investigation may be needed in future. Finally, it is also noteworthy that factors other than biogenic emissions can influence the simulated BVOC mixing ratios over California, such as anthropogenic emissions and the oxidation mechanism of BVOCs used in simulations. Therefore, additional direct measurements of biogenic emission fluxes are needed for a better evaluation of simulated BVOC fluxes.

Chun Zhao 4/29/2016 10:40 AM
Deleted: BVOCs

Chun Zhao 4/29/2016 10:40 AM
Deleted: BVOCs

Code availability

The WRF-Chem version 3.5.1 release can be obtained at http://www2.mmm.ucar.edu/wrf/users/download/get_source.html. Code modifications for implementing MEGANv2.1 into CLM are available upon request by contacting the corresponding author and will be released to public WRF-Chem version.

Acknowledgements

This was work was supported by the U.S. Department of Energy, Office of Science, Office of Biological and Environmental Research's Atmospheric Systems Research (ASR) Program and Atmospheric Radiation Measurement (ARM) Climate Research Facility. A portion of this research was supported by the US NOAA's Atmospheric Composition and Climate Program (NA11OAR4310160). The simulations required for this work were performed on the National Energy Research Scientific Computing Center, supported by the Office of Science of the U.S. Department of Energy. We acknowledge

Dr. Tom Jobson and Dr. Bentram Knighton for their measurements during the CARES campaign. The Pacific Northwest National Laboratory is operated for DOE by Battelle Memorial Institute under contract DE-AC05-76RL01830. NCAR is operated by the University Corporation of Atmospheric Research under sponsorship of the National Science Foundation.

Reference

Andreae, M. and P. J. Crutzen: Atmospheric Aerosols : Biogeochemical Sources and Role in Atmospheric Chemistry. Science, 276, 5315, 1052-1058, doi:10.1126/science.276.5315.1052, 1997.

Arneth, A., S. P. Harrison, S. Zaehle, K. Tsigaridis, S. Menon, P. J. Bartlein, J. Feichter, A. Korhola, M. Kulmala, D. O'Donnell, G. Schurgers, S. Sorvari, and T. Vesala: Terrestrial biogeochemical feedbacks in the climate system, Nature Geoscience, 3, 525-532, 2000.

Arneth, A., Niinemets, Ü., Pressley, S., Bäck, J., Hari, P., Karl, T., Noe, S., Prentice, I. C., Serça, D., Hickler, T., Wolf, A., and Smith, B.: Process‐based estimates of terrestrial ecosystem isoprene emissions: Incorporating the effects of a direct CO2‐isoprene interaction, Atmos. Chem. Phys., 7, 31–53, 2007.

Barlage, M., F. Chen, M. Tewari, K. Ikeda, D. Gochis, J. Dudhia, R. Rasmussen, B. Livneh, M. Ek, and K. Mitchell: Noah land surface model modifications to improve snowpack prediction in the Colorado Rocky Mountains, J. Geophys. Res., 115, D22101, doi:10.1029/2009JD013470, 2010.

Bonan, G. B.: A land surface model (LSM ver. 1.0) for ecological, hydrological, and atmospheric studies: Technical description and user's guide. NCAR Tech. Note 4171STR, 150 pp, 1996.

Bonan, G. B., K. W. Oleson, M. Vertenstein, S. Levis, X. Zeng, Y. Dai, R. E. Dickinson, and Z.-L. Yang: The Land Surface Climatology of the Community Land Model Coupled to the NCAR Community Climate Model. J. Climate, 15, 3123–3149, doi: http://dx.doi.org/10.1175/1520-0442(2002)015<3123:TLSCOT>2.0.CO;2, 2002.

926 Carter,W. P. L.: Documentation of the SAPRC-99 Chemical Mechanism for VOC
927 Reactivity Assessment, Draft report to the California Air Resources Board, Contracts
928 92–329 and 95–308, 8 May, available at: http://www.cert.ucr.edu/~carter/pubs/ (last
929 access:1 December 2015), 2000a.
930 Carter,W. P. L.: Implementation of the SAPRC-99 Chemical Mechanism into the
931 Models-3 Framework, Report to the United States Environmental Protection Agency,
932 29 January, available at: http://www.cert.ucr.edu/~carter/pubs/ (last access: 1
933 December 2015), 2000b.
934 Chameides, W. L., F. Fehsenfeld, M. O. Rodgers, C. Cardelino, J. Martinez, D. Parrish,
935 W. Lonneman, D. R. Lawson, R. A. Rasmussen, P. Zimmerman, J. Greenberg, P.
936 Mlddleton, T. Wang: Ozone precursor relationships in the ambient atmosphere, J.
937 Geophys. Res., 97(D5), 6037–6055, doi:10.1029/91JD03014, 1992.
938 Claeys, M., B. Graham, G. Vas, W. Wang, R. Vermeylen, V. Pashynska, J. Cafmeyer, P.
939 Guyon, M. O. Andreae, P. Artaxo, W. Maenhaut: Formation of Secondary Organic
940 Aerosols Through Photooxidation of Isoprene, Vol. 303 no. 5661 pp. 1173-1176, doi:
941 10.1126/science.1092805, 2004.
942 Cox, P., Delao, A., Komorniczak, A., andWeller, R.: The California almanac of
943 emissions and air quality 2009 edition,
944 http://www.arb.ca.gov/aqd/almanac/almanac09/almanac2009all.pdf, 2009.
945 Dickinson R. E.: Land Surface Processes and Climate Surface Albedos and Energy-
946 Balance. Adv Geophys 25:305-353. doi: 10.1016/S0065-2687(08)60176-4, 1983.

947 Duhl, T. R., Guenther, A., and Helmig, D.: Estimating urban vegetation cover fraction
948 using Google Earth®images, J. Land Use Sci., 7, 311–329,
949 doi:10.1080/1747423X.2011.587207, 2012.
950 Fast, J. D, Gustafson Jr., W. I., Easter, R. C., Zaveri, R. A., Barnard, J. C., Chapman, E.
951 G., and. Grell, G. A.: Evolution of ozone, particulates, and aerosol direct forcing in an
952 urban area using a new fully-coupled meteorology, chemistry, and aerosol model, J.
953 Geophys. Res., 111, D21305, doi:10.1029/2005JD006721, 2006.
954 Fast, J. D., Allan, J., Bahreini, R., Craven, J., Emmons, L., Ferrare, R., Hayes, P. L.,
955 Hodzic, A., Holloway, J., Hostetler, C., Jimenez, J. L., Jonsson, H., Liu, S., Liu, Y.,
956 Metcalf, A., Middlebrook, A., Nowak, J., Pekour, M., Perring, A., Russell, L.,
957 Sedlacek, A., Seinfeld, J., Setyan, A., Shilling, J., Shrivastava, M., Springston, S.,
958 Song, C., Subramanian, R., Taylor, J. W., Vinoj, V., Yang, Q., Zaveri, R. A., and
959 Zhang, Q.: Modeling regional aerosol and aerosol precursor variability over
960 California and its sensitivity to emissions and long-range transport during the 2010
961 CalNex and CARES campaigns, Atmos. Chem. Phys., 14, 10013-10060,
962 doi:10.5194/acp-14-10013-2014, 2014.
963 Fehsenfeld, F., Calvert, J., Fall, R., Goldan, P., Guenther, A.B., Hewitt, C.N., Lamb, B.,
964 Liu, S., Trainer, M., Westberg, H. and Zimmerman, P.: Emissions of volatile organic
965 compounds from vegetation and the implications for atmospheric chemistry. Global
966 Biogeochemical Cycles, 6: doi: 10.1029/92GB02125. issn: 0886-6236, 1992.
967 Gao, Y., X. Liu, C. Zhao, and M. Zhang: Emission controls versus meteorological
968 conditions in determining aerosol concentrations in Beijing during the 2008 Olympic
969 Games, Atmos. Chem. Phys., 11, 12437-12451, 2011.

970 Gao, Y., C. Zhao, X. Liu, M. Zhang, and L. R. Leung: Regional modeling of aerosol and
971 its radiative forcing over East Asia using WRF-Chem, Atmos. Environ., 92, 250-266,
972 2014.
973 Gentner, D. R., Isaacman, G., Worton, D. R., Chan, A. W. H., Dallmann, T. R., Davis, L.,
974 Liu, S., Day, D. A., Russell, L. M., Wilson, K. R., Weber, R., Guha, A., Harley, R.
975 A., and Goldstein, A. H.: Elucidating secondary organic aerosol from diesel and
976 gasoline vehicles through detailed characterization of organic carbon emissions, P.
977 Natl. Acad. Sci. USA, 109, 18318–18323, doi:10.1073/pnas.1212272109, 2012.
978 Greenfield, E.J., D.J. Nowak, and J.T. Walton: Assessment of 2001 NLCD percent tree
979 and impervious cover estimates, Photogrammetric Engineering & Remote Sensing ,
980 75(11): 1279–1286, 2009.
981 Grell, G. A., Peckham, S. E., Schmitz, R., and McKeen, S. A., Frost, G., Skamarock, W.
982 C., and Eder, B.: Fully coupled "online" chemistry within the WRF model, Atmos.
983 Environ., 39, 6957–6976, 2005.
984 Guenther, A. B., P. R. Zimmerman, P. C. Harley, R. K. Monson, and R. Fall: Isoprene
985 and monoterpene emission rate variability: model evaluations and sensitivity
986 analyses. Journal of Geophysical Research, vol. 98, no. 7, pp. 12–617, 1993.
987 Guenther, A. B., Hewitt, C. N., Erickson, D., Fall, R., Geron, C., Graedel, T., Harley, P.,
988 Klinger, L., Lerdau, M., McKay, W. A., Pierce, T., Scholes, B., Steinbrecher, R.,
989 Tallamraju, R., Taylor, J., and Zimmerman, P.: A global model of natural volatile
990 organic compound emissions, J. Geophys. Res.-Atmos., 100, 8873–8892, 1995.
991 Guenther, A. B., W. Baugh, K. Davis, Gary Hampton, P. Harley, L. Klinger, L. Vierling,
992 P. Zimmerman, E. Allwine, S. Dilts, B. Lamb, H. Westberg, D. Baldocchi, C. Geron,

993 T. Pierce: Isoprene fluxes measured by enclosure, relaxed eddy accumulation, surface
994 layer gradient, mixed layer gradient, and mixed layer mass balance techniques.
995 Journal of Geophysical Research D, vol. 101, no. 13, pp. 18555–18567, 1996.
996 Guenther, A., T. Karl, P. Harley, C. Wiedinmyer, P. I. Palmer, and C. Geron: Estimates
997 of global terrestrial isoprene emissions using MEGAN (Model of Emissions of Gases
998 and Aerosols from Nature). Atmospheric Chemistry and Physics, vol. 6, no. 11, pp.
999 3181–3210, 2006.
1000 Guenther, A. B., Jiang, X., Heald, C. L., Sakulyanontvittaya, T., Duhl, T., Emmons, L.
1001 K., and Wang, X.: The Model of Emissions of Gases and Aerosols from Nature
1002 version 2.1 (MEGAN2.1): an extended and updated framework for modeling biogenic
1003 emissions, Geosci. Model Dev., 5, 1471-1492, doi:10.5194/gmd-5-1471-2012, 2012.
1004 Guenther, A. B.: Biological and chemical diversity of biogenic volatile organic emissions
1005 into the atmosphere, ISRN Atmospheric Sciences, 2013, 786290, 1-27, 2013.
1006 Hong, Song-You, Yign Noh, Jimy Dudhia: A new vertical diffusion package with an
1007 explicit treatment of entrainment processes. Mon. Wea. Rev., 134, 2318–2341, 2006.
1008 Huang, M., Carmichael, G. R., Spak, S. N., Adhikary, B., Kulkarni, S., Cheng, Y., Wei,
1009 C., Tang, Y., D'Allura, A., Wennberg, P. O., Huey, G. L., Dibb, J. E., Jimenez, J. L.,
1010 Cubison, M. J., Weinheimer, A. J., Kaduwela, A., Cai, C., Wong, M., Bradley Pierce,
1011 R., Al-Saadi, J. A., Streets, D. G., and Zhang, Q.: Multi-scale modeling study of the
1012 source contributions to near-surface ozone and sulfur oxides levels over California
1013 during the ARCTAS-CARB period, Atmos. Chem. Phys., 11, 3173-3194,
1014 doi:10.5194/acp-11-3173-2011, 2011.

1015 Hijmas, R. J., S. E. Cameron, J. L. Parra, P. G. Jones, and A. Jarvis: Very high resolution
1016 interpolated climate surfaces for global land areas. Int. J. Climatol. 25: 1965–1978
1017 (2005), DOI: 10.1002/joc.1276, 2005.
1018 Iacono, M. J., J. S. Delamere, E. J. Mlawer, M. W. Shephard, S. A. Clough, and W. D.
1019 Collins: Radiative forcing by long–lived greenhouse gases: Calculations with the
1020 AER radiative transfer models. J. Geophys. Res., 113, D13103, 2008.
1021 Jin, J., and N. L. Miller (2007), Analysis of the impact of snow on dailyweather
1022 variability in mountainous regions using MM5, J. Hydrometeorol.,8, 245 –258,
1023 doi:10.1175/JHM565.1.
1024 Jin, J., and L. Wen: Evaluation of snowmelt simulation in the Weather Research and
1025 Forecasting model, J. Geophys. Res., 117, D10110, doi:10.1029/2011JD016980,
1026 2012.
1027 Kain, John S.: The Kain–Fritsch convective parameterization: An update. J. Appl.
1028 Meteor., 43, 170–181, 2004.
1029 Ke Y, LYR Leung, M Huang, AM Coleman, H Li, and MS Wigmosta: Development of
1030 High Resolution Land Surface Parameters for the Community Land Model.
1031 Geoscientific Model Development 5(6):1341-1362. doi:10.5194/gmd-5-1341-2012,
1032 2012.
1033 Knote, C., Hodzic, A., Jimenez, J. L., Volkamer, R., Orlando, J. J., Baidar, S., Brioude,
1034 J., Fast, J., Gentner, D. R., Goldstein, A. H., Hayes, P. L., Knighton, W. B., Oetjen,
1035 H., Setyan, A., Stark, H., Thalman, R., Tyndall, G., Washenfelder, R., Waxman, E.,
1036 and Zhang, Q.: Simulation of semi-explicit mechanisms of SOA formation from

glyoxal in aerosol in a 3-D model, Atmos. Chem. Phys., 14, 6213-6239, doi:10.5194/acp-14-6213-2014, 2014.

Lamb, B., A. Guenther, D. Gay, H. Westberg: A national inventory of biogenic hydrocarbon emissions. Atmos. Environ., 21, 8, 1695-1705, doi:10.1016/0004-6981(87)90108-9, 1987.

Lawrence, P.J. and T.N. Chase: Climate Impacts. Our earth's changing land: an encyclopedia of land-use and land-cover change, H. Geist, Greenwood Press, Westport, 115-124, 2006.

Lawrence, P. J. and T. N. Chase: Representing a new MODIS consistent land surface in the Community Land Model (CLM 3.0). J. Geophys. Res.-Biogeosci.: Vol. 112, 2007.

Lawrence, D.M., K.W. Oleson, M.G. Flanner, P.E. Thornton, S.C. Swenson, P.J. Lawrence, X. Zeng, Z.-L. Yang, S. Levis, K. Sakaguchi, G.B. Bonan, and A.G. Slater: Parameterization improvements and functional and structural advances in version 4 of the Community Land Model. J. Adv. Model. Earth Sys., 3, DOI: 10.1029/2011MS000045, 2011.

Lemone, M. A., F. Chen, M. Tewari, J. Dudhia, B. Geerts, Q. Miao, R. L. Coulter, and R. L. Grossman (2010a), Simulating the IHOP_2002 Fair-Weather CBL with the WRF-ARW-Noah modeling system. Part I: Surface fluxes and CBL structure and evolution along the eastern track, Mon. Weather Rev., 138(3), 722–744, doi:10.1175/2009mwr3003.1.

Lemone, M. A., F. Chen, M. Tewari, J. Dudhia, B. Geerts, Q. Mia, R. L. Coulter, and R. L. Grossman (2010b), Simulating the IHOP_2002 Fair-Weather CBL with the WRF-

ARW Noah modeling system. Part II: Structures from a few kilometers to 100 km across, Mon. Weather Rev., 138(3), 745–764, doi:10.1175/2009mwr3004.1.

Lindinger, W., Hansel, A., and Jordan, A.: On-line monitoring of volatile organic compounds at pptv levels by means of protontransfer-reaction mass spectrometry (PTR-MS) – medical applications, food control and environmental research, Int. J. Mass Spectrom., 173, 191–241, 1998.

McKeen, S. A., G. Wotawa, D. D. Parrish, J. S. Holloway, M. P. Buhr, G. Hubler, F. C. Fehsenfeld, and J. F. Meagher: Ozone production from Canadian wildfires during June and July of 1995, J. Geophys. Res., 107(D14), 4192, doi:10.1029/2001JD000697, 2002.

Morrison, H., G. Thompson, V. Tatarskii: Impact of Cloud Microphysics on the Development of Trailing Stratiform Precipitation in a Simulated Squall Line: Comparison of One– and Two–Moment Schemes. Mon. Wea. Rev., 137, 991–1007, 2009.

Müller J.-F.: Geographical distribution and seasonal variation of surface emissions and deposition velocities of atmospheric trace gases. J. Geophys. Res. 97(D4): 3787-3804, 1992.

Niinemets, Ü., J. D. Tenhunen, P. C. Harley, and R. Steinbrecher: A model of isoprene emission based on energetic requirements for isoprene synthesis and leaf photosynthetic properties for Liquidambar and Quercus, Plant Cell Environ., 22, 1319–1335, 1999.

Chun Zhao 4/29/2016 10:40 AM
Deleted: veloci- ties

Chun Zhao 4/29/2016 10:40 AM
Deleted: –

1083 Niinemets, Ü., G. Seufert, R. Steinbrecher, and J. D. Tenhunen: A model coupling foliar
1084 monoterpene emissions to leaf photosynthetic characteristics in Mediterranean
1085 evergreen Quercus species, New Phytol., 153, 257–275, 2002.
1086 Oleson, K. W., Lawrence, D. M., Bonan, G. B., Flanner, M. G., Kluzek, E., Lawrence, P.
1087 J., Levis, S., Swenson, S. C., Thornton, P. E., Dai, A., Decker, M., Dickinson, R.,
1088 Feddema, J., Heald, C. L., Hoffman, F., Lamarque, J.-F., Mahowald, N., Niu, G.-Y.,
1089 Qian, T., Randerson, J., Running, S., Sakaguchi, K., Slater, A., Sto¨ckli, R., Wang,
1090 A., Yang, Z.-L., Zeng, X., and Zeng, X.: Tech- nical Description of version 4.0 of the
1091 Community Land Model (CLM), Tech. Rep. NCAR/TN-478 + STR, National Center
1092 for Atmospheric Research, 2010.
1093 Oliver Wild, Xin Zhu, Michael J. Prather: Fast-J: Accurate Simulation of In- and Below-
1094 Cloud Photolysis in Tropospheric Chemical Models, J. Atmos. Chem., Volume 37,
1095 Issue 3, pp 245-282, 2000.
1096 Paulson, C. A.: The mathematical representation of wind speed and temperature profiles
1097 in the unstable atmospheric surface layer. J. Appl. Meteor., 9, 857–861, 1970.
1098 Pfister, G. G., Parrish, D. D.,Worden, H., Emmons, L. K., Edwards, D. P., Wiedinmyer,
1099 C., Diskin, G. S., Huey, G., Oltmans, S. J., Thouret, V., Weinheimer, A., and
1100 Wisthaler, A.: Characterizing summertime chemical boundary conditions for air
1101 masses entering the US West Coast, Atmos. Chem. Phys., 11, 1769–1790,
1102 doi:10.5194/acp-11-1769-2011, 2011.
1103 Pierce, T., C. Geron, L. Bender, R. Dennis, G. Tonnesen, and A. Guenther: Influence of
1104 increased isoprene emissions on regional ozone modeling, J. Geophys. Res.,
1105 103(D19), 25611–25629, doi:10.1029/98JD01804, 1998.

1106 Poisson, N., M. Kanakidou, P. J. Crutzen: Impact of Non-Methane Hydrocarbons on
1107 Tropospheric Chemistry and the Oxidizing Power of the Global Troposphere: 3-
1108 Dimensional Modelling Results, J. Atmos. Chem., 36, 157-230, 2000.
1109 Rasmussen, R. A.: What do the hydrocarbons from trees contribute to air pollution? J. Air
1110 Poll. Con. Asso., 22, 7, 537-543, 1972.
1111 Ryerson, T. B., Andrews, A. E., Angevine, W. M., Bates, T. S., Brock, C. A., Cairns, B.,
1112 Cohen, R. C., Cooper, O. R., de Gouw, J. A., Fehsenfeld, R. C., Ferrare, R. A.,
1113 Fischer, M. L., Flagan, R. C., Goldstein, A. H., Hair, J. W., Hardesty, R. M.,
1114 Hostetler, C. A., Jimenez, J. L., Langford, A. O., McCauley, E., McKeen, S. A.,
1115 Molina, L. T., Nenes, A., Oltmans, S. J., Parrish, D. D., Pederson, J. R., Pierce, R. B.,
1116 Prather, K., Quinn, P. K., Seinfeld, J. H., Senff, C. J., Sorooshian, A., Stutz, J.,
1117 Surratt, J. D., Trainer, M., Volkamer, R., Williams, E. J., and Wofsy, S. C.: The 2010
1118 California Research at the Nexus of Air Quality and Climate Change (CalNex) field
1119 study, J. Geophys. Res., 118, 5830-5866, doi:10.1002/jgrd.50331, 2013.
1120 Sakulyanontvittaya, T., Duhl, T., Wiedinmyer, C., Helmig, D., Mat- sunaga, S.,
1121 Potosnak, M., Milford, J., and Guenther, A.: Monoter- pene and sesquiterpene
1122 emission estimates for the United States, Environ. Sci. Technol., 42, 1623–1629,
1123 2008.
1124 Sanderson, M.G., Jones, C.D., Collins, W.J., Johnson, C.E. and Derwent, R.G.: Effect of
1125 Climate Change on Isoprene Emissions and Surface Ozone Levels. Geophysical
1126 Research Letters 30: doi: 10.1029/2003GL017642. issn: 0094-8276, 2003.

1127 Schurgers, G., A. Arneth, R. Holzinger, and A. Goldstein: Processbased modelling of
1128 biogenic monoterpene emissions combining production and release from storage,
1129 Atmos. Chem. Phys., 9, 3409–3423, 2009.
1130 Shilling, J. E., R. A. Zaveri, J. D. Fast, L. I. Kleinman, M. L. Alexander, M. R.
1131 Canagaratna, E. Fortner, J. M. Hubbe, J. T. Jayne, A. Sedlacek, A. Setyan, S.
1132 Springston, D. R. Worsnop, and Q. Zhang: Enhanced SOA formation from mixed
1133 anthropogenic and biogenic emissions during the CARES campaign. Atmospheric
1134 Chemistry and Physics, 13(4):2091-2113, doi:10.5194/acp-13-2091-2013, 2013.
1135 Shrivastava MKB, JD Fast, RC Easter, Jr, WI Gustafson, Jr, RA Zaveri, JL Jimenez, P
1136 Saide, and A Hodzic: Modeling Organic Aerosols in a Megacity: Comparison of
1137 Simple and Complex Representations of the Volatility Basis Set Approach.
1138 Atmospheric Chemistry and Physics 11(13):6639-6662. doi:10.5194/acp-11-6639-
1139 2011.
1140 Shrivastava MKB, A Zelenyuk, D Imre, RC Easter, Jr, J Beranek, RA Zaveri, and JD
1141 Fast: Implications of Low Volatility SOA and Gas-Phase Fragmentation Reactions on
1142 SOA Loadings and their Spatial and Temporal Evolution in the Atmosphere. Journal
1143 of Geophysical Research. D. (Atmospheres), 118(8), 3328-3342,
1144 doi:10.1002/jgrd.50160, 2013.
1145 Stauffer, D. R. and Seaman, N. L.: Use of four-dimensional data assimilation in a limited-
1146 area mesoscale model, Part I: Experiments with synoptic-scale data, Mon. Weather
1147 Rev., 118, 1250–1277, 1990.

1148 Still, C. J., J. A. Berry, G. J. Collatz, and R. S. DeFries, Global distribution of C3 and C4
1149 vegetation: Carbon cycle implications, Global Biogeochem. Cycles, 17(1), 1006,
1150 doi:10.1029/2001GB001807, 2003.
1151 Went, F. W.: blue hazes in the atmosphere, Nature, Vol. 187, 4738, 641-643, 1960.
1152 Wild, O., X. Zhu, and Prather, M. J.: Fast-J: Accurate simulation of in- and below-cloud
1153 photolysis in tropospheric chemical models. Journal of Atmospheric Chemistry,
1154 37(3), 245 - 282. doi: 10.1023/A:1006415919030, 2000.
1155 Willmott, C. J. and K. Matsuura: Terrestrial Air Temperature and Precipitation: Monthly
1156 and Annual Time Series (1950 - 1999), 2011
1157 (http://climate.geog.udel.edu/~climate/html_pages/README.ghcn_ts2.html).
1158 Zaveri, R. A., Shaw, W. J., Cziczo, D. J., Schmid, B., Ferrare, R. A., Alexander, M. L.,
1159 Alexandrov, M., Alvarez, R. J., Arnott, W. P., Atkinson, D. B., Baidar, S., Banta, R.
1160 M., Barnard, J. C., Beranek, J., Berg, L. K., Brechtel, F., Brewer, W. A., Cahill, J. F.,
1161 Cairns, B., Cappa, C. D., Chand, D., China, S., Comstock, J. M., Dubey, M. K.,
1162 Easter, R. C., Erickson, M. H., Fast, J. D., Floerchinger, C., Flowers, B. A., Fortner,
1163 E., Gaffney, J. S., Gilles, M. K., Gorkowski, K., Gustafson, W. I., Gyawali, M., Hair,
1164 J., Hardesty, R. M., Harworth, J. W., Herndon, S., Hiranuma, N., Hostetler, C.,
1165 Hubbe, J. M., Jayne, J. T., Jeong, H., Jobson, B. T., Kassianov, E. I., Kleinman, L. I.,
1166 Kluzek, C., Knighton, B., Kolesar, K. R., Kuang, C., Kubátová, A., Langford, A. O.,
1167 Laskin, A., Laulainen, N., Marchbanks, R. D., Mazzoleni, C., Mei, F., Moffet, R. C.,
1168 Nelson, D., Obland, M. D., Oetjen, H., Onasch, T. B., Ortega, I., Ottaviani, M.,
1169 Pekour, M., Prather, K. A., Radney, J. G., Rogers, R. R., Sandberg, S. P., Sedlacek,
1170 A., Senff, C. J., Senum, G., Setyan, A., Shilling, J. E., Shrivastava, M., Song, C.,

Springston, S. R., Subramanian, R., Suski, K., Tomlinson, J., Volkamer, R., Wallace, H. W., Wang, J., Weickmann, A. M., Worsnop, D. R., Yu, X.-Y., Zelenyuk, A., and Zhang, Q.: Overview of the 2010 Carbonaceous Aerosols and Radiative Effects Study (CARES), Atmos. Chem. Phys., 12, 7647-7687, doi:10.5194/acp-12-7647-2012, 2012.

Zeng, X., M. Shaikh, Y. Dai, R. E. Dickinson, and R. Myneni (2002), Cou-pling of the common land model to the NCAR community climate model,J. Clim., 15, 1832–1854, doi:10.1175/1520-0442(2002)015<1832:COTCLM>2.0.CO;2.

Zhao, C., Hu, Z., Qian, Y., Ruby Leung, L., Huang, J., Huang, M., Jin, J., Flanner, M. G., Zhang, R., Wang, H., Yan, H., Lu, Z., and Streets, D. G.: Simulating black carbon and dust and their radiative forcing in seasonal snow: a case study over North China with field campaign measurements, Atmos. Chem. Phys., 14, 11475-11491, doi:10.5194/acp-14-11475-2014, 2014.

Zimmerman, P. R., R. B. Chatfield, J. Fishman, P. J. Crutzen, and P. L. Hanst, Estimates the production of CO and H2 from the oxidation of hydrocarbon emissions from vegetation, Geophys. Res. Lett., 5, 679-682, 1978.

Zimmerman, P.: Testing of hydrocarbon emissions from vegetation, leaf litter and aquatic surfaces and development of a method for compiling biogenic emission inventories, Tech. Rep. EPA-450-4-70-004, U.S. Environmental Protection Agency, Research Triangle Park, California, USA, 1979.

Table 1 Average percentage of PFTs over the simulation domain

PFT # and description		USGS	VEG1	VEG2	VEG3
0	Bare soil	26.0	7.6	38.1	41.6
1	Needleleaf evergreen tree – temperate	13.0	12.5	9.1	10.7
2	Needleleaf evergreen tree - boreal	0.0	0.1	0.0	4.9
3	Needleleaf deciduous tree – boreal	0.1	0.0	0.0	0.0
4	Broadleaf evergreen tree – tropical	0.0	0.0	0.0	0.0
5	Broadleaf evergreen tree – temperate	0.0	0.4	1.9	0.0
6	Broadleaf deciduous tree – tropical	2.9	0.0	0.0	0.0
7	Broadleaf deciduous tree – temperate	1.5	0.4	1.8	1.5
8	Broadleaf deciduous tree – boreal	0.0	0.0	0.0	0.3
9	Broadleaf evergreen shrub - temperate	21.1	5.3	0.0	0.3
10	Broadleaf deciduous shrub – temperate	20.0	37.5	27.4	10.8
11	Broadleaf deciduous shrub – boreal	0.9	0.2	0.0	1.0
12	C_3 arctic grass	0.0	0.0	1.2	2.2
13	C_3 grass	1.0	28.0	14.9	18.9
14	C_4 grass	10.4	0.0	0.0	0.0
15	Crop	3.2	6.5	4.1	6.3

[1]USGS is the 16-PFT dataset converted from the default 24 USGS land cover dataset based on a lookup table derived from Bonan et al. [1996];
[2]VEG1 is from the PFT fractional cover product by Ke et al. [2012];
[3]VEG2 is obtained from the NCAR CESM data repository [Oleson et al., 2010];
[4]VEG3 is derived from a dataset over the U.S. with 16 PFT classifications by combining the National Land Cover Dataset (NLCD, Homer et al., 2004) and the Cropland Data Layer (see http://nassgeodata.gmu.edu/CropScape/).

Table 2 Experiments of WRF-Chem

	Surface scheme	BVOC scheme	Plant Function Type Dataset				
			USGS/VEG-M	USGS	VEG1	VEG2	VEG3
WRF-Chem	CLM4.0	MEGANv2.0 MEGANv2.1	Mv20CLM -	- Mv21USGS	- Mv21V1	- Mv21V2	- Mv21V3
	Noah	MEGANv2.0	Mv20Noah	-	-	-	-

Chun Zhao 4/29/2016 10:40 AM
Deleted: PFT's

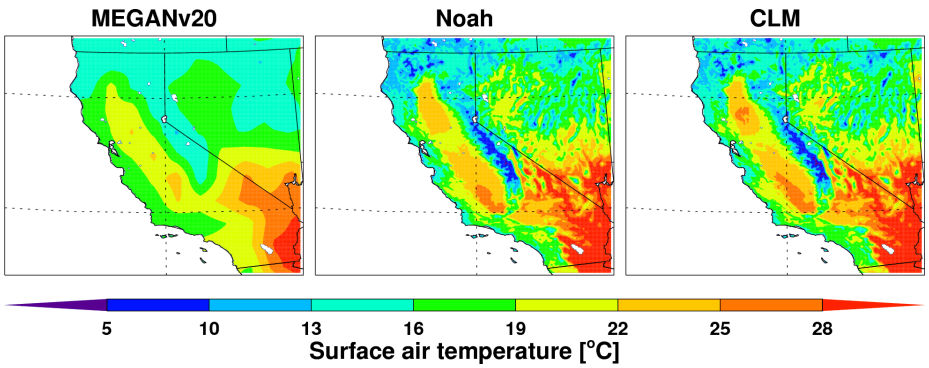

Figure 1 Spatial distributions of monthly mean surface air temperature in June 2010 from the MEGAN v2.0 climatology dataset (MEANv20, prescribed) and the WRF-Chem simulations with the Noah (Noah, simulated) and CLM4 (CLM, simulated) land surface schemes.

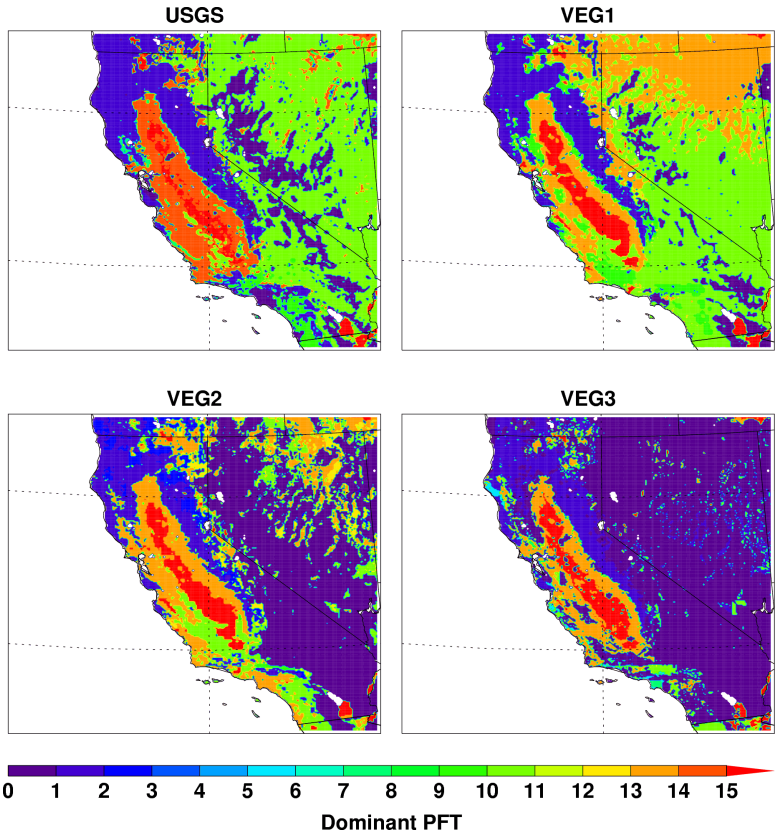

Figure 2. Spatial distribution of dominant PFTs over the simulation domain from the four datasets: USGS, VEG1, VEG2, and VEG3. The PFT number is referred to the list in Table 1.

Chun Zhao 4/29/2016 10:40 AM
Deleted: PFT's

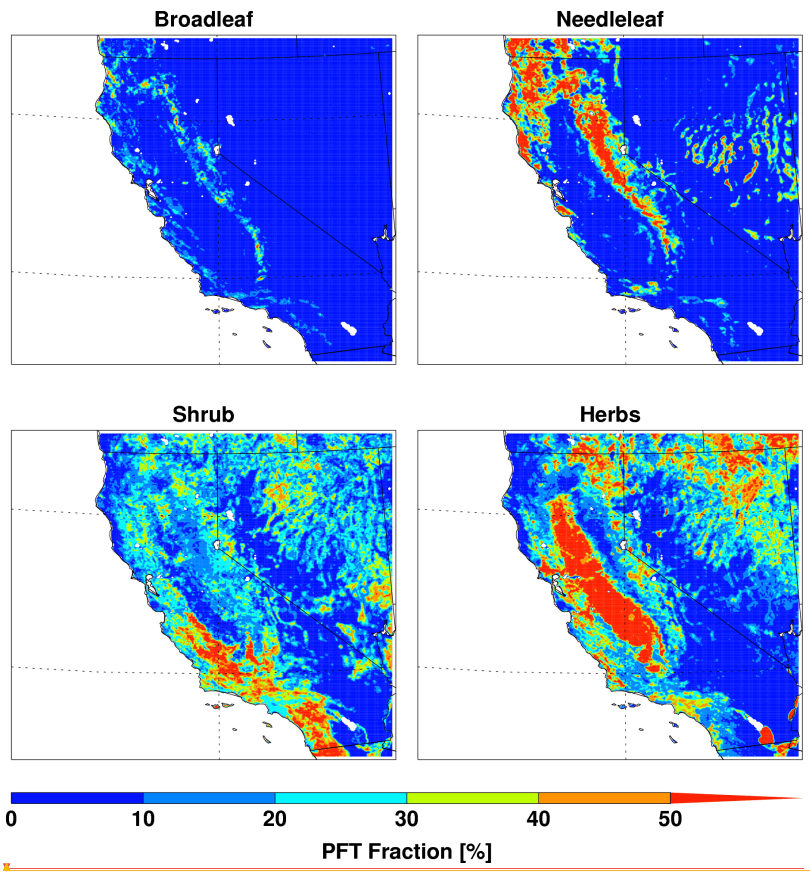

Figure 3.

Chun Zhao 4/29/2016 10:40 AM
Formatted: Font:Bold

Chun Zhao 4/29/2016 10:40 AM
Deleted: ... [1]

Unknown
Formatted: Font:Times New Roman

Unknown
Formatted: Font:Times New Roman, Bold

Chun Zhao 4/29/2016 10:40 AM
Moved down [2]: is referred to the list in Table 1.

Spatial distribution of percentage of the four PFTs from the VEG-M used by MEGAN v2.0 over the simulation domain.

Chun Zhao 4/29/2016 10:40 AM
Deleted: . ... [2]
Unknown
Formatted: Font:Times New Roman, Bold

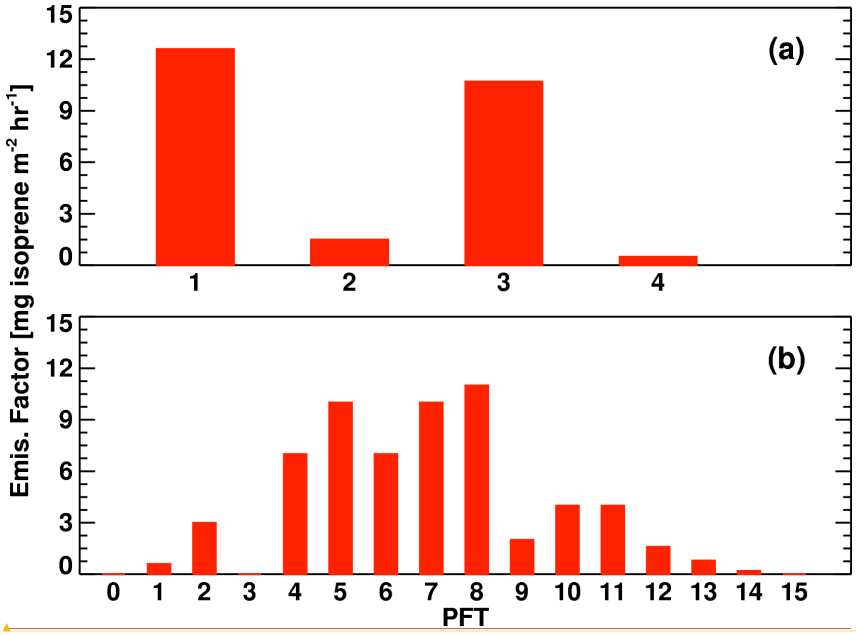

Figure 4. Biogenic isoprene emission factor for each PFT in (a) MEGAN v2.0, the PFT number 1-4 is referred to Broadleaf, Needleleaf, Shrub, and Herbs, respectively; (2) MEGAN v2.1, the PFT number 0-15 is referred to the list in Table 1.

Unknown
Formatted: Font:Times New Roman

Chun Zhao 4/29/2016 10:40 AM
Moved (insertion) [2]

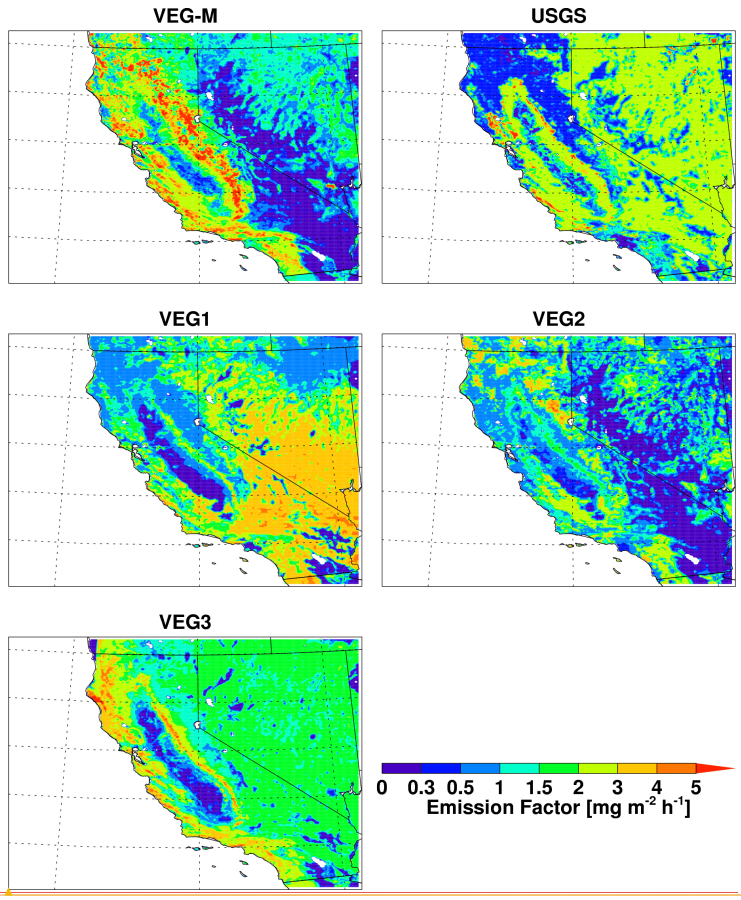

Chun Zhao 4/29/2016 10:40 AM
Deleted: ... [3]
Unknown
Formatted: Font:Times New Roman
Unknown
Formatted: Font:Times New Roman

Figure 5. Spatial distribution of PFT-weighted mean biogenic isoprene emission factor derived with the VEG-M in MEGAN v2.0 and the USGS, VEG1, VEG2, and VEG3 in MEGAN v2.1.

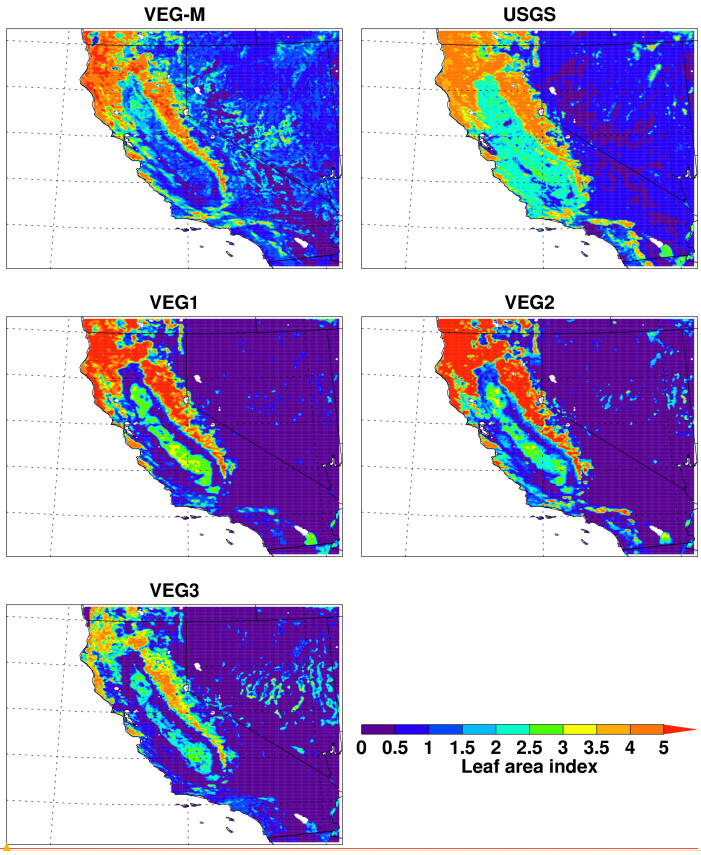

Figure 6. Spatial distribution of leaf area index (LAI) from the VEG-M in MEGAN v2.0 and from the USGS, VEG1, VEG2, and VEG3 in MEGAN v2.1.

Unknown
Formatted: Font:Times New Roman, Bold

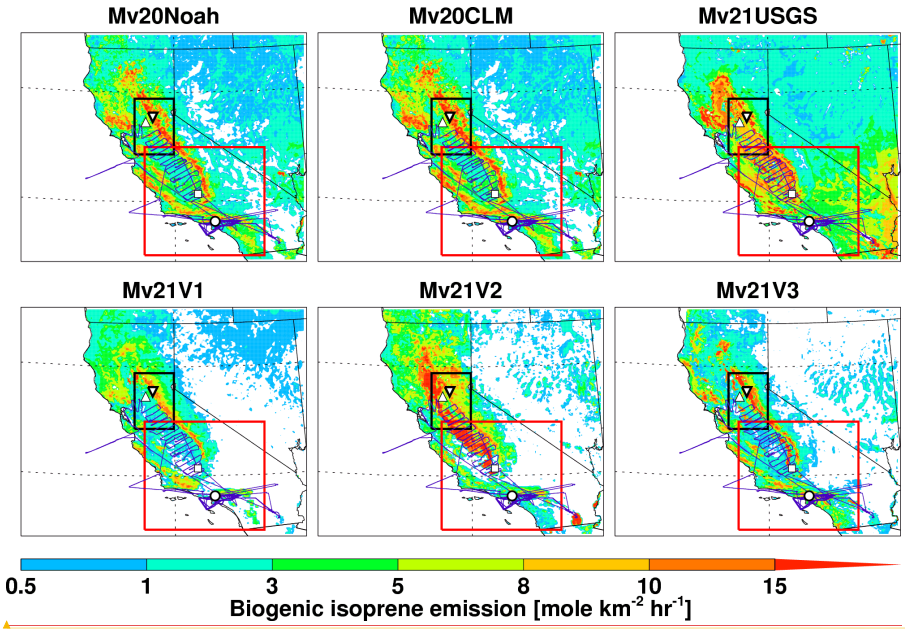

Unknown
Formatted: Font:Times New Roman

Figure 7. Spatial distributions of biogenic isoprene emissions averaged in June estimated in the six simulations as listed in Table 2. The four observation sites are shown as T0 (white upward triangle), T1 (white downward triangle), Bakersfield (white square), and Pasadena (white circle). The CalNex WP-3D flight tracks below 1 km (blue line) during June 2010 are also shown. The black and red boxes denote the predominant CARES and CalNex regions, respectively.

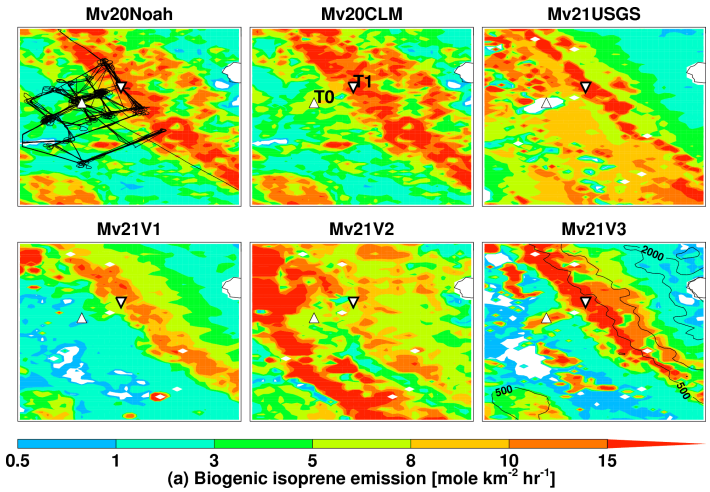

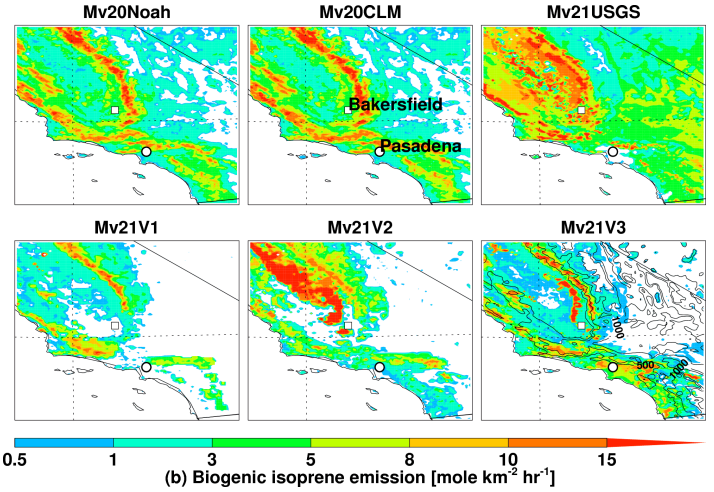

Figure 8. a) Spatial distributions of biogenic isoprene emissions around the CARES observational sites T0 and T1 (the black box shown in Fig. 7) estimated in the six simulations as listed in Table 1. The CARES G-1 flight tracks below 1 km (black line) during June 2010 are also shown with the Mv20Noah result; the terrain height is also shown as the black contour lines with the Mv21V3 result. b) Same as a) except around the CalNex observational sites Bakersfield and Pasadena (the red box shown in Fig. 7).

Chun Zhao 4/29/2016 10:40 AM
Deleted: 6

Chun Zhao 4/29/2016 10:40 AM
Deleted: 5

Chun Zhao 4/29/2016 10:40 AM
Deleted: 5

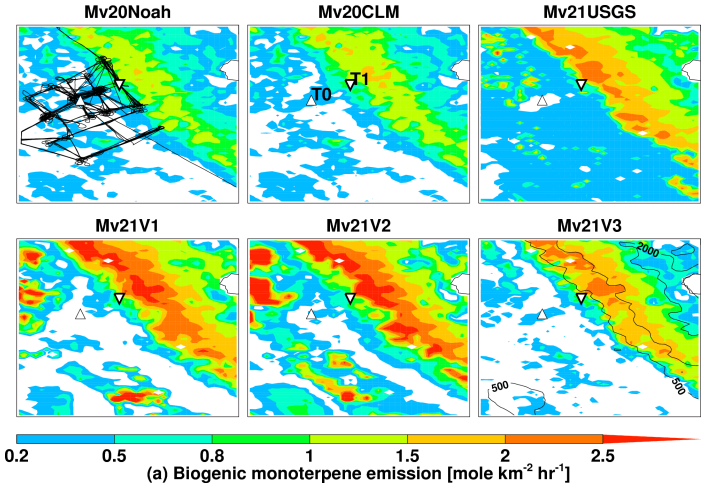

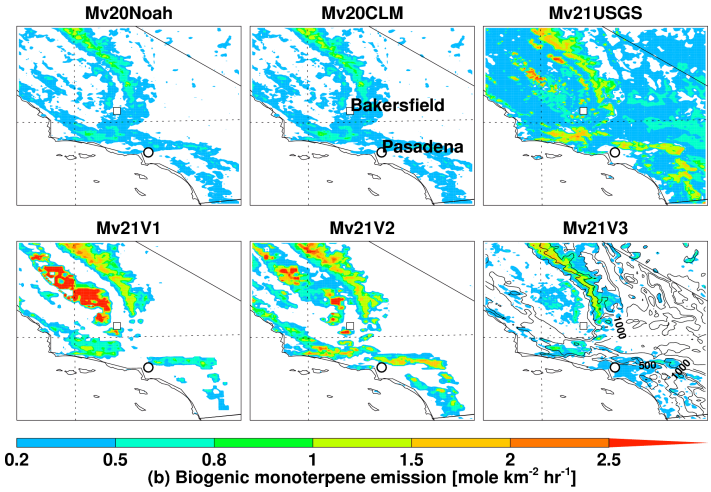

Figure 9. Same as Fig. 8, except for biogenic monoterpene emissions.

Chun Zhao 4/29/2016 10:40 AM
Deleted: 7

Chun Zhao 4/29/2016 10:40 AM
Deleted: 6

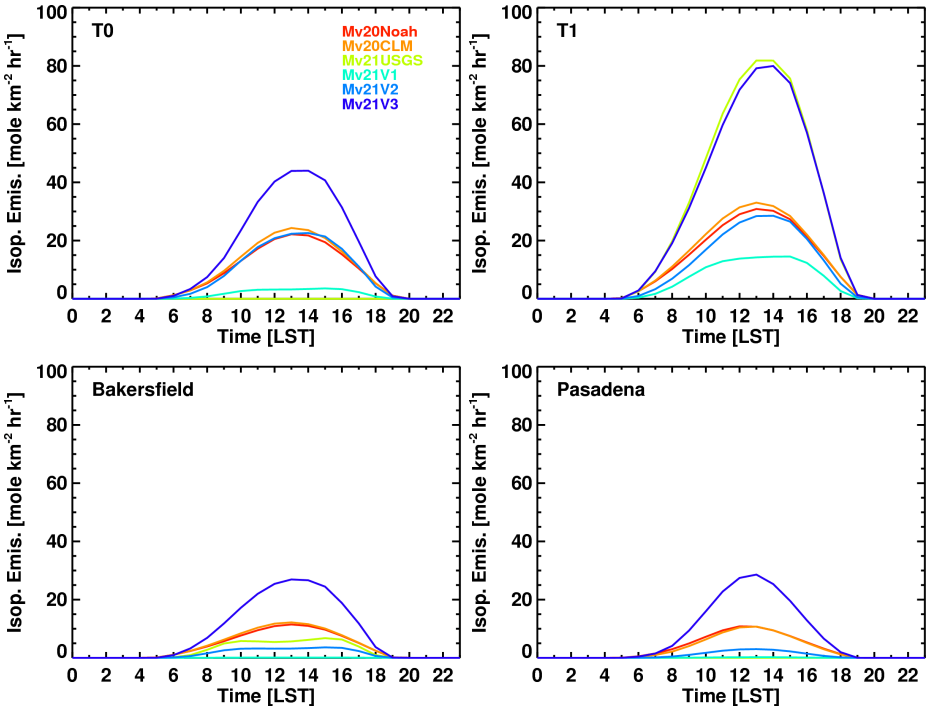

Figure 10. Average diurnal variation of biogenic isoprene emissions at the four observation sites from the six simulations listed in Table 1.

Chun Zhao 4/29/2016 10:40 AM
Deleted: 8

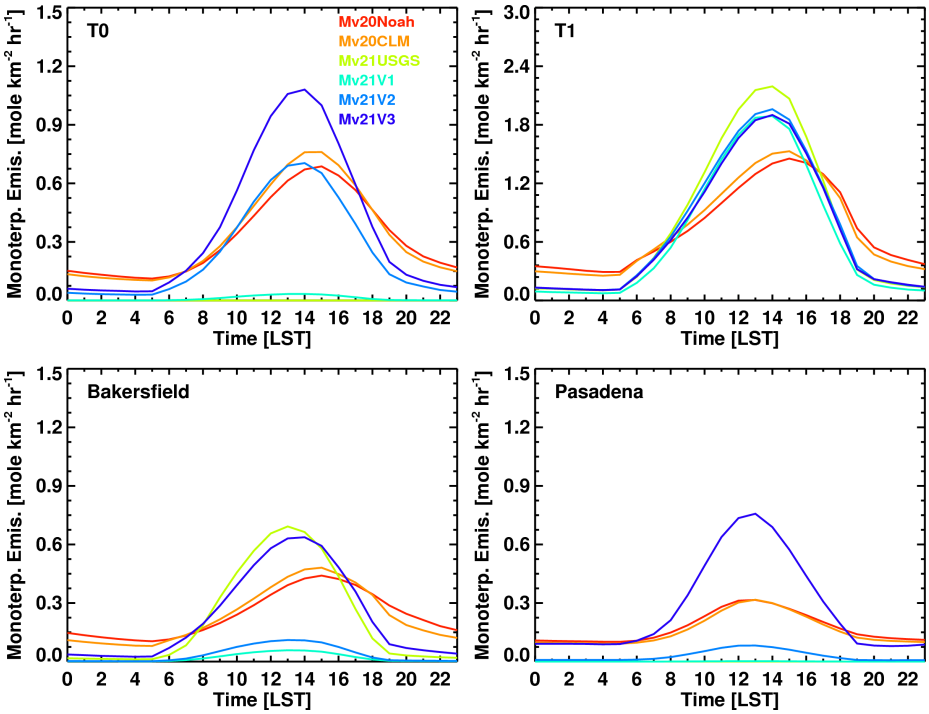

Figure 11. Same as Fig. 10, except for biogenic monoterpene emissions.

Chun Zhao 4/29/2016 10:40 AM
Deleted: 9

Chun Zhao 4/29/2016 10:40 AM
Deleted: 8

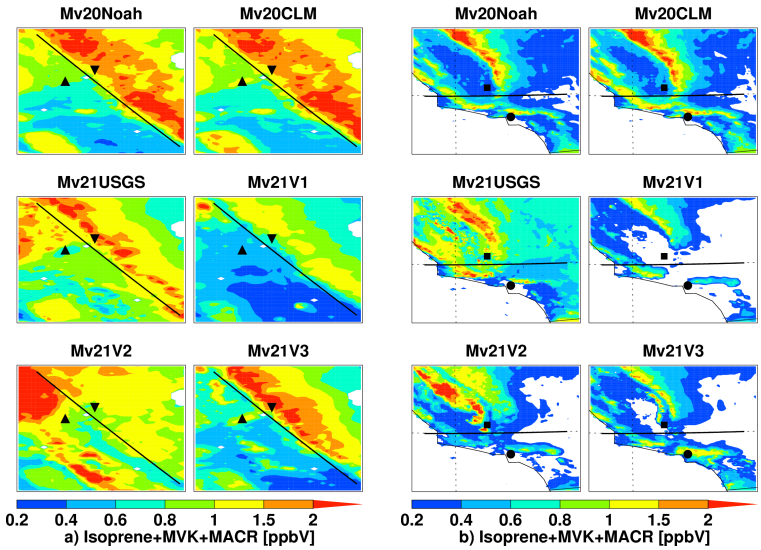

Figure 12. a) Spatial distributions of monthly averaged surface isoprene mixing ratios around the CARES T0 and T1 observational sites from the six simulations as listed in Table 1. The black lines parallel to the Sierra Nevada divide the region to the Southwest and the Northeast for comparison with CARES G-1 aircraft measurements shown in Fig. 16 and 17. b) Same as a) except around the CalNex observational sites Bakersfield and Pasadena. The black lines divide the region to southern California and the Central Valley for comparison with CalNex WP-3D aircraft measurements shown in Fig. 16 and 17.

Chun Zhao 4/29/2016 10:40 AM
Deleted: 10

Chun Zhao 4/29/2016 10:40 AM
Deleted: 14

Chun Zhao 4/29/2016 10:40 AM
Deleted: 15

Chun Zhao 4/29/2016 10:40 AM
Deleted: 14

Chun Zhao 4/29/2016 10:40 AM
Deleted: 15

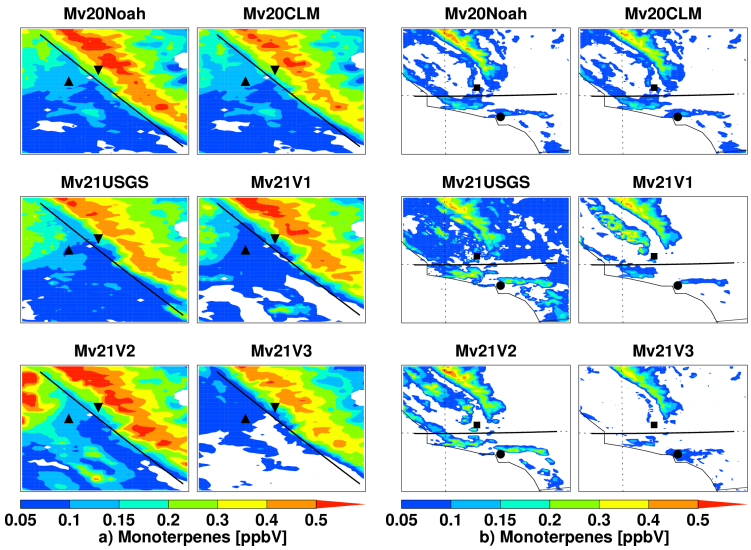

Figure 13. Same as Fig. 12, except for monoterpene.

Chun Zhao 4/29/2016 10:40 AM
Deleted: 11

Chun Zhao 4/29/2016 10:40 AM
Deleted: 10

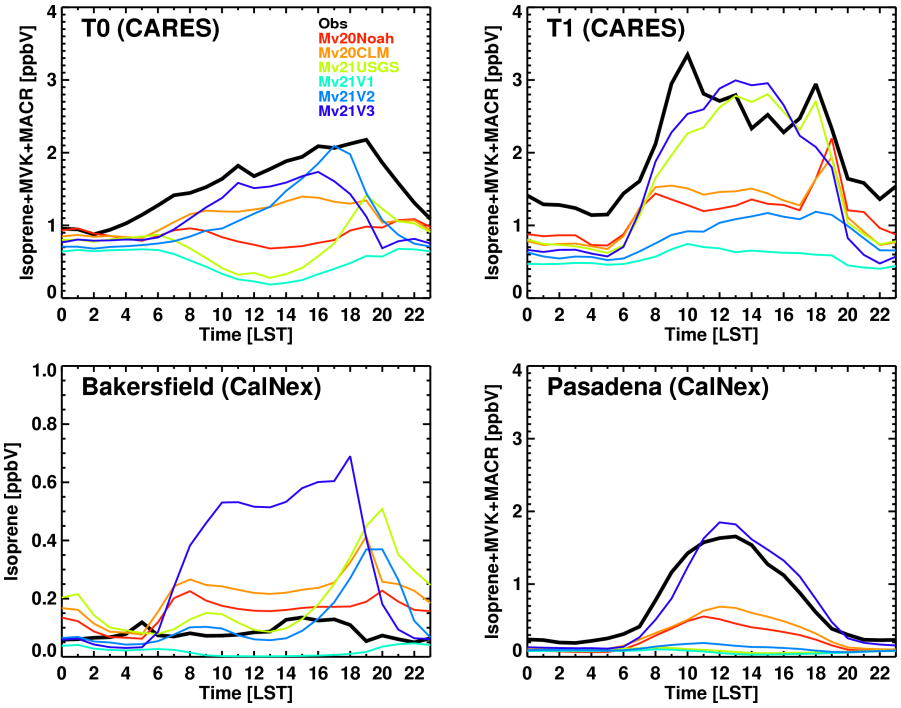

Figure 14. Monthly averaged diurnal variation of surface isoprene+MVK+MACR mixing ratios at the three observation sites and isoprene mixing ratios at the Bakersfield site from the observations and six simulations listed in Table 2. The simulated values for the Bakersfield and Pasadena sites are averaged for the first two weeks of June to be consistent with the observations.

Chun Zhao 4/29/2016 10:40 AM
Deleted: 12

Chun Zhao 4/29/2016 10:40 AM
Deleted: four

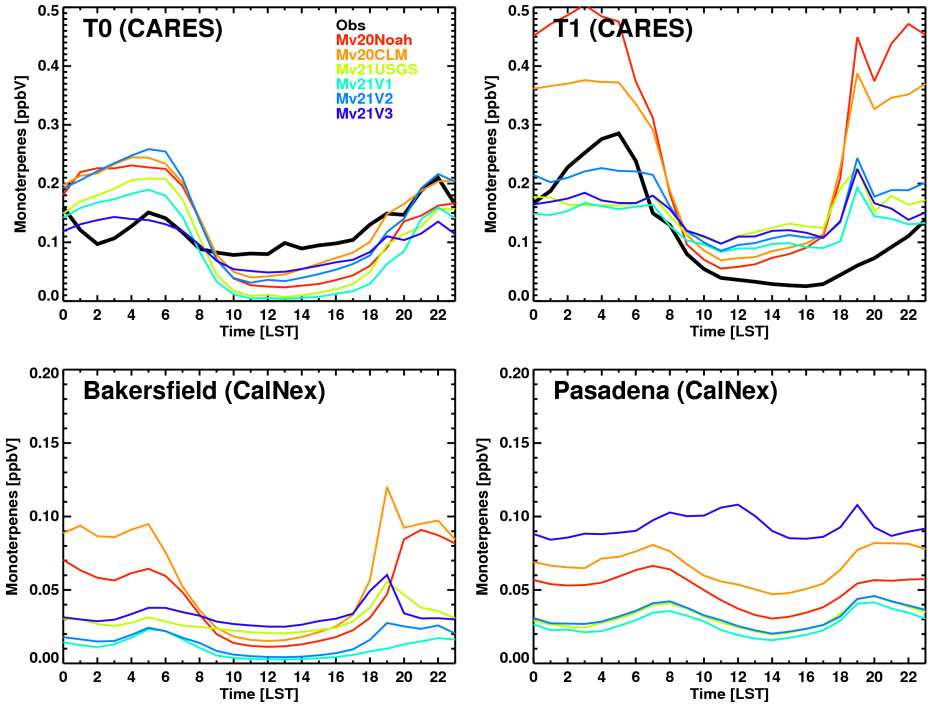

Figure 15. Monthly averaged diurnal variation of surface monoterpene mixing ratios at the four observation sites from the observations and six simulations as listed in Table 2. There are no observations for the Bakersfield and Pasadena sites in June.

Chun Zhao 4/29/2016 10:40 AM
Deleted: 13

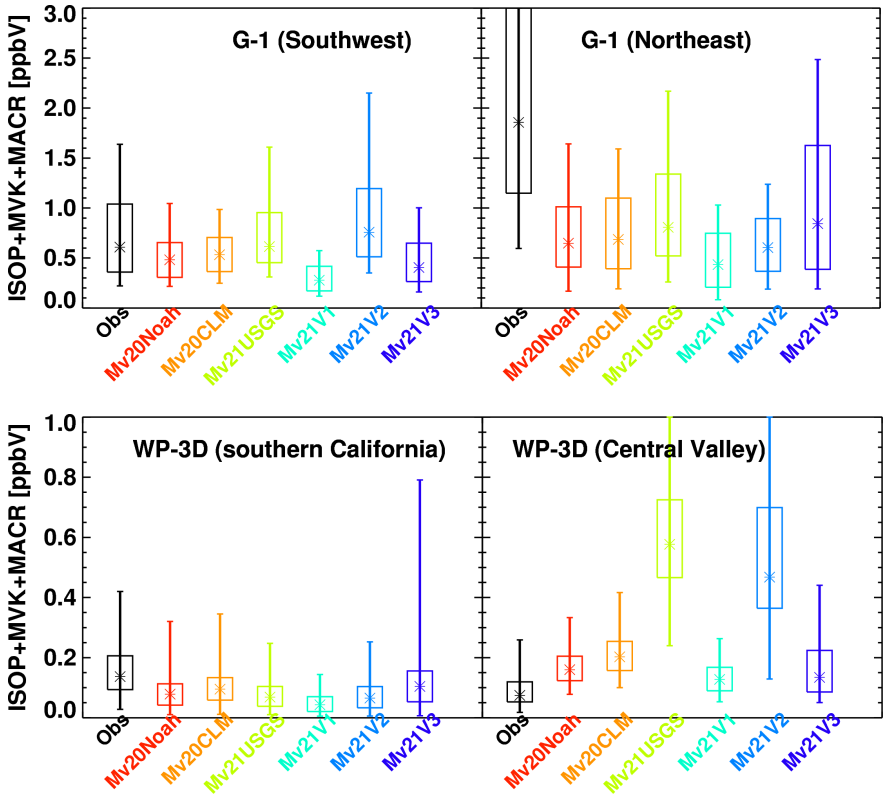

Figure 16. Comparison of isoprene+MVK+MACR mixing ratios averaged below 1 km from the observations by G-1 flights over the Southwest and Northeast regions (as marked in Fig. 12a) and WP-3D flights over southern California and the Central Valley (as marked in Fig. 12b) and the corresponding simulations. Asterisk denotes the 50th percentiles. Vertical lines denote 10th and 90th percentiles, and the boxes denote the 25th and 75th percentiles.

Chun Zhao 4/29/2016 10:40 AM
Deleted: 14

Chun Zhao 4/29/2016 10:40 AM
Deleted: 10a

Chun Zhao 4/29/2016 10:40 AM
Deleted: 10b

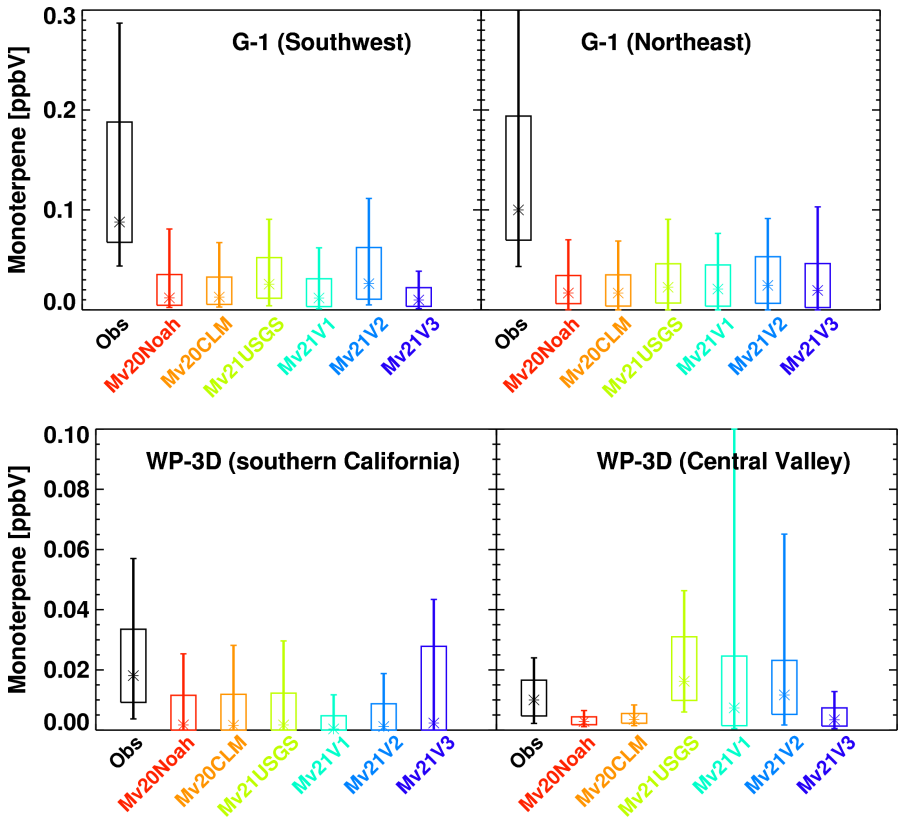

Figure 17. Same as Fig. 16 except for monoterpene mixing ratios.

Chun Zhao 4/29/2016 10:40 AM
Deleted: 15

Chun Zhao 4/29/2016 10:40 AM
Deleted: 14

Page 51: [1] Deleted Chun Zhao 4/29/16 10:40 AM

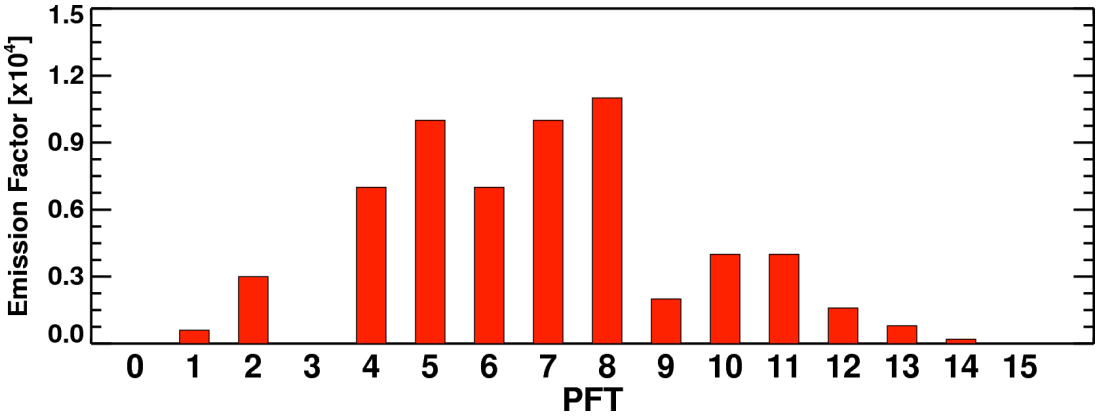

Figure 3. Biogenic isoprene emission factor for each PFT in MEGAN v2.1. The PFT number

Page 52: [2] Deleted Chun Zhao 4/29/16 10:40 AM

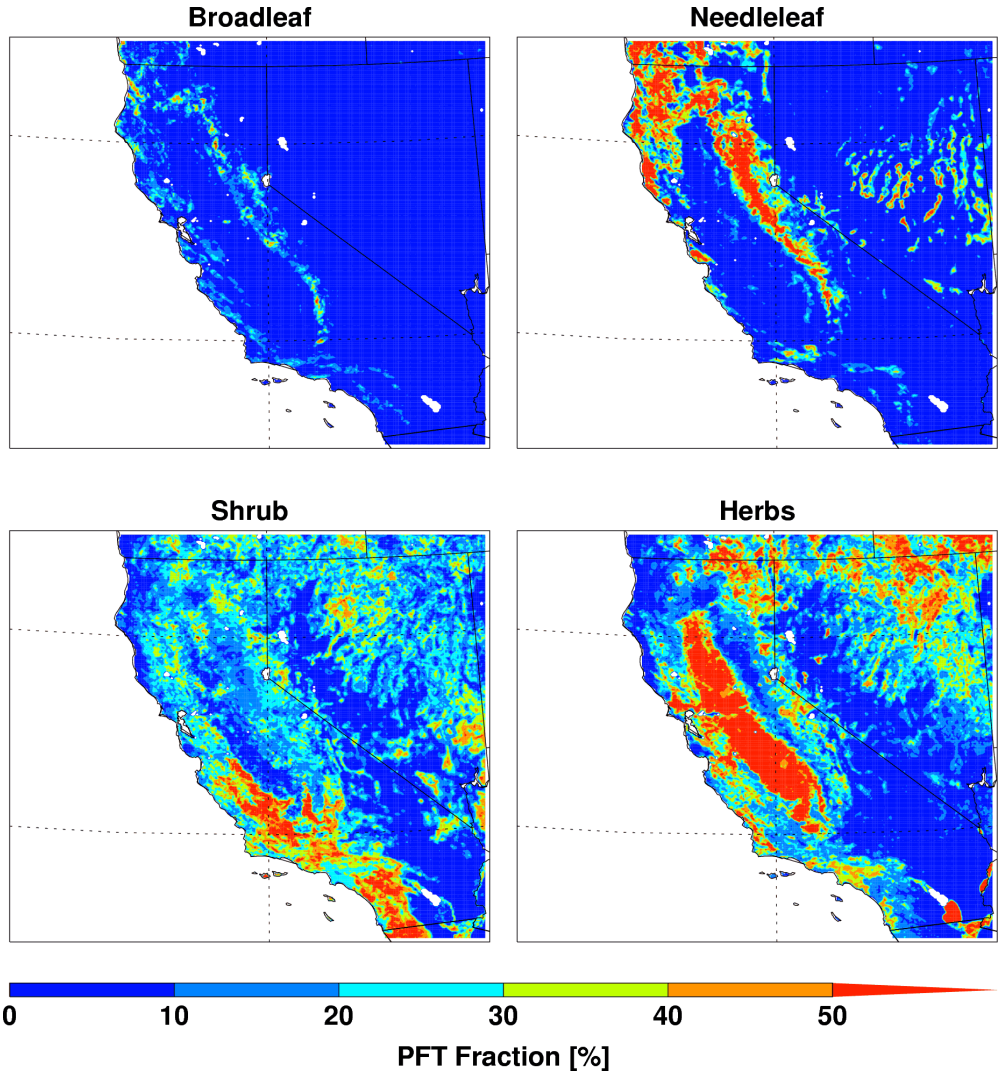

Figure 4.

Page 54: [3] Deleted Chun Zhao 4/29/16 10:40 AM

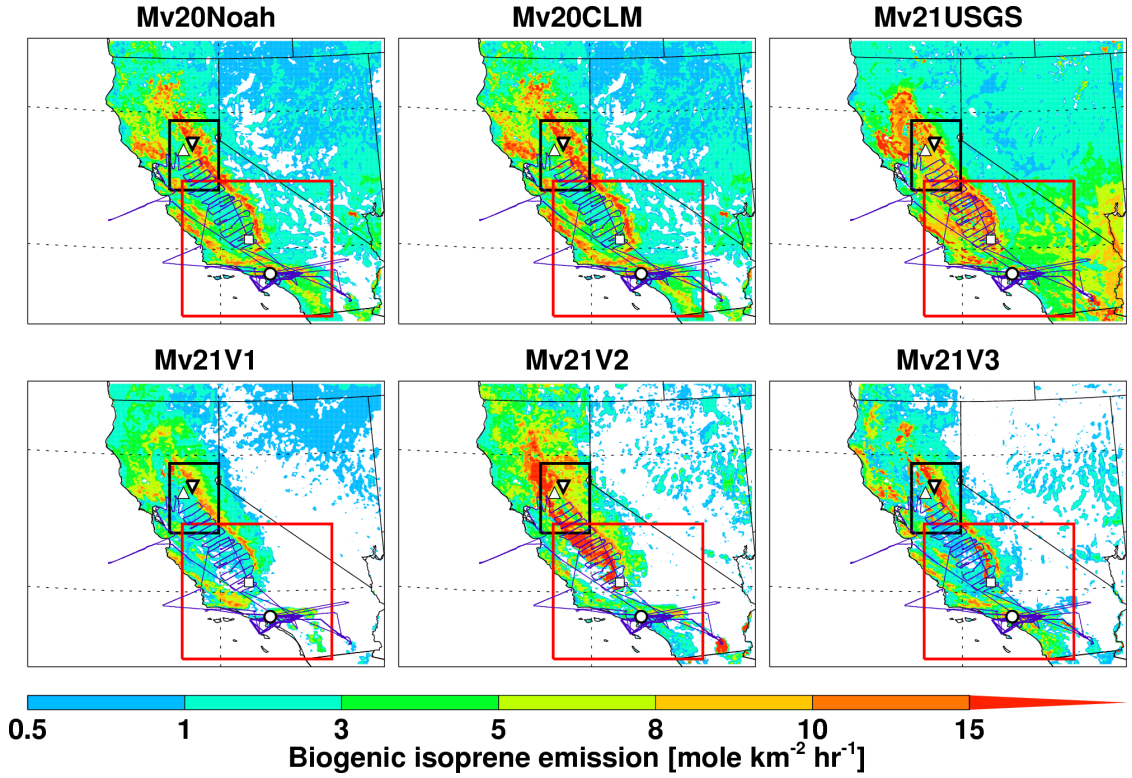
Mv20Noah
Mv20CLM
Mv21USGS
Mv21V1
Mv21V2
Mv21V3
0.5
1
3
5
8
10
15
Biogenic isoprene emission [mole km-2 hr-1]

Figure 5.